NEXT GENERATION WEATHER RADAR PROGRAM

OPERATIONAL SUPPORT FACILITY

Dual-Polarization Radar Fundamentals and Algorithm Prospects

Edward A. Brandes
National Center for Atmospheric Research
Research Applications Program
Boulder, Colorado

12 MAY 2000

TABLE OF CONTENTS

OVERVIEW

Dual-polarization radars typically transmit horizontally and vertically polarized electromagnetic waves and receive polarized backscattered signals. Because illuminated hydrometeors are not exactly spherical, their radar backscatter cross sections are not the same for the different polarizations. Electromagnetic waves propagating through precipitation typically are subject to scattering, differential attenuation, differential phase shifts, and depolarization. Signal properties change continuously as the wave propagates yielding information that can be used to estimate particle size, shape, orientation, and thermodynamic phase. The measurements should lead to improved rainfall estimation, hail detection, rain-snow discrimination, and data quality. Potential new capabilities include general hydrometeor classification and a capacity to discriminate between meteorological and biological targets.

The purpose of this report is to provide an introduction to radar polarimetry–the theory and physical basis for the measurements–and to discuss possible applications (algorithms). [Important supplements to this discussion are given by Oguchi (1983), Bringi and Hendry (1990), Zrnić (1991), and Doviak and Zrnić (1993); algorithm prospects are also discussed by Zrnić et al. (1999).] The report is organized as follows: Section 1 reviews properties of hydrometeor distributions. A brief review of the backscattering and backscattering covariance matrices follows (Section 2). Common radar-measured and derived quantities are discussed in Section 3. Possible applications including rainfall estimation, hail and bright band detection, hydrometeor discrimination, and data quality assessment are described in Section 4. A concluding section (Section 5) summarizes key findings and recommends that a committee be established to develop an evaluation plan for possible implementation on the WSR-88D.

1. PARTICLE DISTRIBUTIONS

Because they have been studied extensively, the discussion in this section focusses on the distribution of raindrops in the atmosphere. However, the described distributions have been shown to be roughly applicable to other precipitation types (hail and snow) as well. The growth of raindrops is determined largely by collision and coalescence processes which reduce the number of small drops and shift the distribution to larger drops. Growth is countered by breakup once the drops reach a certain size. Marshall and Palmer (1948) determined experimentally that drop distributions at equilibrium could be described by an exponential relation of the form

$$N(D) = N_0 \exp(-\Lambda D) \quad (1)$$

where D is the drop diameter [mm], N(D) is the number density of the drops per unit volume [mm^{-1} m^{-3}], N_0 is the zero intercept [mm^{-1} m^{-3}], and Λ is the slope of the distribution [mm^{-1}]. The slope was related to the rainfall rate R [mm h^{-1}] by

$$\Lambda = 4.1\ R^{-0.21} \quad . \qquad [mm^{-1}]$$

Marshall and Palmer determined that

$$N_0 = 8000 \quad . \qquad [mm^{-1}\ m^{-3}]$$

Consequently,

$$N(D) = 8000 \exp(4.1\ R^{-0.21}\ D) \quad . \qquad [mm^{-1}\ m^{-3}]$$

Observed drop-size distributions (DSDs) often exhibit fewer small and fewer large drops than predicted by Eq.1. Hence, Ulbrich (1983) proposed a gamma distribution

$$N(D) = N_0\ D^{\mu} \exp(-\Lambda D) \qquad (2)$$

where μ is a distribution shape parameter. A positive (negative) value of μ results in a distribution with relatively fewer (more) small and large drops than Eq. 1, i.e., the distribution turns concave downward (upward) when log[N(D)] is plotted versus D. With Eq. 2, N_0 is no longer the intercept of the distribution but a parameter proportional to the concentration.

It is often assumed that the exponential distribution is most applicable to stratiform precipitation and longer time periods and that the gamma distribution is more representative of shorter time periods and more convective rainfalls. Importantly, the exponential distribution has two governing parameters (N_0 and Λ); and the gamma distribution has three parameters (N_0, Λ, and μ). Successful application requires two and three radar measurements, respectively.

DSD parameters can vary greatly. Ulbrich (1983) found that μ varied approximately from -3 to 5 and N_0 varied roughly from 10^2 to 10^7. Observational studies (e.g., Waldvogel 1974; Atlas et al. 1999; Tokay and Short 1996; Illingworth and Johnson 1999) suggest parameter ranges of

$$10^2 \le N_0 \le 10^{12} \qquad [mm^{-1-\mu}\ m^{-3}]$$
$$2 \le \Lambda \le 20 \qquad [mm^{-1}]$$
$$-2 \le \mu \le 12 \quad .$$

The relative frequency of particular parameter values has not been determined. In general, as the rain rate increases, there is a tendency for N_0 to decrease, often to values less than that of Marshall-Palmer. Slope and shape parameters also tend to decrease in magnitude with rain rate.

A useful parameter in radar meteorology is the median volume diameter (D_0) defined as

$$\int_0^{D_0} D^3 N(D)\, dD = \int_{D_0}^{D_{max}} D^3 N(D)\, dD \quad .$$

One half of the liquid water content is contained in droplets smaller and one half in drops larger than D_0. The median volume diameter is readily related to other DSD parameters. For example, Atlas (1953) found that $\Lambda D_0 = 3.75$ for an exponential distribution. Sekhon and Srivastava (1970) altered this relation slightly to $\Lambda D_0 = 3.67$ (for $D_{max}/D_0 > 2.5$). For a gamma DSD, $\Lambda D_0 = 3.67 + \mu$ (Ulbrich 1983).

Polarimetric measurements make use of the fact that raindrops tend to flatten as they fall. In still air raindrops fall with an "equilibrium shape" that results when the forces that act upon the drop (surface tension, hydrostatic pressure, aerodynamic pressure, and internal circulation) are in balance. The drops assume a "hamburger bun" shape where the degree of flattening increases with drop size. Wind tunnel experiments conducted by Pruppacher and Beard (1970) indicate that

$$a/b = 1.03 - 0.062\, D$$

where a/b is the ratio of the minor and major axes and D (in mm) is the equivalent volume (spherical) diameter of drops $\geq$ 1 mm. Green (1975) used a hydrostatic drop model and determined that

$$D = 20[\sigma/(g\rho)]^{1/2}(b/a)^{1/6}[(b/a)^2 - 2(b/a)^{1/3} + 1]^{1/2}$$

where $\sigma = 72.75$ g s^{-2}, g = 980 cm s^{-2}, and $\rho = 0.998$ g cm^{-3}. Green's equilibrium ratios closely agree with those of Pruppacher and Beard. Both relations are widely used for comparing simulated and observed DSDs with radar measurements. Some evidence from radar measurements suggests that small drops may be more spherical than implied from these relations (Section 4.1).

2. DUAL-POLARIZATION MEASUREMENTS

Interest here is on the linear horizontal (H)-vertical (V) polarization basis which is likely to be chosen for the WSR-88D (Doviak et al. 2000). Other polarization bases, e.g., circularly and elliptically polarizations, are possible and have different properties (see Bringi and Hendry 1990; Doviak and Zrnić 1993).

The American Heritage Dictionary defines polarization as "the production or condition of polarity, as the uniform and nonrandom elliptical, circular, or linear variation of a wave characteristic, especially of vibrational orientation, in light or other radiation". Weather radars typically transmit linearly polarized electromagnetic energy in which the electric vector oscillates in a specified plane. As the electromagnetic wave propagates through precipitation, it is subject to attenuation, phase shift, and depolarization as well as scattering. How the wave is altered depends upon the size, shape, orientation, and thermodynamic phase of illuminated

hydrometeors. Raindrops fall with their major axes in the horizontal. Pristine ice crystals have significant axial ratios and also fall with their major axes in the horizontal. Hail, graupel, and snow aggregates tend to tumble giving a random distribution of particle orientations as they fall. Media properties can be deduced by transmitting and receiving radar signals with known polarization. For meteorological targets, hydrometeor discrimination is facilitated by operation at horizontal and vertical polarizations.

Radar signals contain a backscattering component which relates to hydrometeor properties within a particular measurement volume (e.g., reflectivity, differential reflectivity, correlation coefficient) and a propagation component that accumulates along the radar beam (e.g., attenuation, differential phase shifts, depolarization). There may also be a backscatter differential phase shift due to the presence of non-Rayleigh (Mie) particles larger than about one tenth of the radar wavelength.

2.1 Backscattering matrix

Transmitted (incident) and the backscattered (reflected) electric fields are related by the scattering matrix S which for a single scatterer (following the notation of Zrnić (1991) and Doviak and Zrnić 1993) can be written

$$\begin{matrix} s_{hh} & s_{hv} \\ s_{vh} & s_{vv} \end{matrix} .$$

By convention the first index refers to the polarization of the backscattered electric field and the second index refers to the transmitted energy. The complex elements of the backscattering matrix are fundamental to the meteorological interpretation of the radar returns. Their magnitudes are determined by the size, shape, and composition of illuminated particles and the radar frequency. The terms s_{hh} and s_{vv} represent co-polar scattering processes where the polarizations of transmitted and returned energy are the same. The terms s_{vh} and s_{hv} arise from transformations whereby a small amount of the transmitted energy leaks into the orthogonal polarization. Precipitation is considered to be a reciprocal medium; hence, it is assumed that $s_{vh} = s_{hv}$.

2.2 Backscattering covariance matrix

Radars actually measure voltages which are related to the elements of the backscattering matrix. The voltages are composed of wave forms which have zero mean when summed over an ensemble of drops. Consequently, second order moments are used to characterize the polarized signals. The backscattering elements comprise a covariance matrix, which after removing reciprocal terms reduces to

$$\begin{array}{lll} \langle |s_{hh}|^2 \rangle & \langle s_{hv} s^*_{hh} \rangle & \langle s_{vv} s^*_{hh} \rangle \\ \langle s_{hh} s^*_{hv} \rangle & \langle |s_{hv}|^2 \rangle & \langle s_{vv}{}^* s_{hv} \rangle \\ \langle s_{hh} s^*_{vv} \rangle & \langle s_{hv} s^*_{vv} \rangle & \langle |s_{vv}|^2 \rangle \end{array} \quad .$$

Brackets $\langle\ \rangle$ denote expected values for an ensemble of particles. The diagonal terms are real, and the six off-diagonals terms are complex conjugates. The nine terms constitute the full suite of parameters that can be generated under the assumption that $s_{vh} = s_{hv}$. Six measurements are required, the three diagonal and three off-diagonal terms.

3. MEASURED AND DERIVED POLARIMETRIC PARAMETERS [1]

In this section we review the properties of radar reflectivities at horizontal polarization (Z_h) and vertical polarization (Z_v), differential reflectivity (Z_{DR}), correlation coefficient (ρ_{hv}), linear depolarization ratio (LDR), and differential phase (ϕ_{DP}). We also briefly discuss two other correlations (ρ_{xh} and ρ_{xv}) whose utility is only now being determined and a derived parameter–the difference reflectivity (Z_{DP}). [For detailed descriptions readers should consult Doviak and Zrnić (1993, Chapter 8).]

3.1 Radar reflectivity factor (Z_h and Z_v)

The radar reflectivity factor per unit volume at horizontal polarization (Z_h) is defined as

$$Z_h = \int_0^{D_{max}} N(D)\, D_h^6\, dD$$

where D_h is the particle dimension in the horizontal direction as seen by the radar. Radar reflectivity has units of $mm^6\ m^{-3}$. The reflectivity at horizontal polarization expressed in terms of the covariance element s_{hh} is

$$Z_h = (4\lambda^4/\pi^4 |K|^2)\langle |s_{hh}|^2 \rangle$$

where λ is the radar wavelength and $|K|^2$, the dielectric factor, is a constant related to the complex index of refraction m by $K = (m^2 - 1)/(m^2 + 2)$. The constant for water, $|K_w|^2$, is 0.93; for ice $|K_i|^2$ is 0.176 at a density of 0.92 g cm^{-3}. Because the dielectric factor is usually included in the "radar constant", it is important to account for phase changes whenever rainfall is estimated from radar reflectivity measurements obtained above the freezing level. The

[1] In the discussion which follows the radar reflectivity factors Z_h and Z_h are understood to represent co-polar measurements in which the polarization of the transmitted and returned energy is the same.

expressions for reflectivity factor at vertical polarization (Z_v) are

$$Z_v = \int_0^{D_{max}} N(D) D_v^6 dD \quad ,$$

where D_v is the radar-sensed particle dimension in the vertical, and

$$Z_v = (4\lambda^4/\pi^4|K|^2)\langle|s_{vv}|^2\rangle \quad .$$

Reflectivity is most often expressed in dBZ ($10\log Z_{h,v}$). Because radar reflectivity is proportional to the number of particles and to the 6th power of their diameters, reflectivity is most sensitive to particle size. A factor of 2 increase in diameter corresponds to an 18 dB increase in reflectivity; a factor of 2 increase in particle concentration raises the reflectivity by only 3 dB. For typical weather radars the standard error of individual reflectivity measurements is ±1 dB. Typical values of reflectivity factor for various precipitation types, as given by Doviak and Zrnić (1993), are presented in Table 1. An example of a vertical cross section of radar reflectivity through a severe hail storm is shown in Fig. 1.

3.2 Differential reflectivity (Z_{DR})

The differential reflectivity (Z_{DR}, in dB), computed from the radar reflectivity at horizontal and vertical polarization, is given by

$$Z_{DR} = 10\log(Z_h/Z_v) \quad .$$

An alternate form, in terms of scattering covariance elements, is

$$Z_{DR} = 10\log(\langle|s_{hh}|^2\rangle/\langle|s_{vv}|^2\rangle) \quad .$$

Raindrops flatten while falling and orient themselves with their major axes close to horizontal in the mean. Thus, for rain Z_h is greater than Z_v. Z_{DR} for convective rainfalls typically ranges between 0.5 and 4 dB (Table 1, Fig. 1 near ground between 52 and 70 km) and generally increases with rainfall intensity. Light rainfalls with reflectivity values of 20 to 30 dBZ often have differential reflectivities of 0.1 to 0.5 dB. Pristine ice crystals falling with their major axes near horizontal have a differential reflectivity of 0 to 5 dB depending on the crystal type. For anisotropic particles (i.e., hydrometeors with a preferred orientation such as raindrops or pristine ice crystals) Z_{DR} is a measure of reflectivity-weighted oblateness or axis ratio. The refractive index, related to the complex index of refraction, is ~9 for water and 1.78 for ice (Battan 1973, Chapter 4). Consequently, at a particular axis ratio a water droplet has a larger Z_{DR} than an ice particle (see, e.g., Seliga and Bringi 1976). Aggregates,

graupel, and hail tend to tumble as they fall. For a fully random (isotropic) distribution of hydrometer orientations Z_h and Z_v would be equal, and Z_{DR} would be 0 dB. But typically signatures for tumbling particles vary from small negative to small positive values. [For the hail shaft in Fig. 1 (near 51 km), Z_{DR} at ground is 0.5 to 1.0 dB.]

As a ratio of reflectivity factors, Z_{DR} is relatively insensitive to hardware calibration and is insensitive to the number concentration parameter N_0. [Attributes of the common polarimetric parameters are summarized in Table 2.] Verification of the Z_{DR} measurement is accomplished by pointing the radar vertically and rotating the antenna through 360° to avoid direction dependent bias associated with ground clutter (Gorgucci et al. 1999a). Raindrops, when viewed in this manner should have a Z_{DR} of 0 dB. Light rainfall should have a small positive value of Z_{DR} close to 0 dB at all viewing angles. The standard error of the Z_{DR} measurement, as indicated by gate-to-gate scatter among measurements along a radial is on the order of 0.2 to 0.3 dB. This error can be reduced to ~0.1 dB by spatial averaging. Errors of this magnitude are important for rainfall estimation when Z_{DR} is small.

Potential uses for Z_{DR} include estimating rainfall (Section 4.2.3), hail detection (Section 4.3.1), discriminating between liquid and frozen precipitation (Sections 4.5 and 4.6), and detecting biological scatterers (Zrnić and Ryzhkov 1998). Differential reflectivity measurements are susceptible to ground clutter and sidelobe contamination and may be biased by mismatches between the horizontal and vertical beams of the radar. Hail contributes dominantly to the Z_{DR} measurement when mixed with rain. Also, heavy rainfall and hail can cause significant differential attenuation and create a negative bias in Z_{DR}.

3.3 Linear depolarization ratio (LDR_{hv} and LDR_{vh})

Hydrometeors whose principal axes are not aligned with the electrical field of the transmitted wave cause a small amount of energy to be depolarized and to appear at the orthogonal polarization. The effect is measured by the linear depolarization ratio (LDR, in dB), defined as the ratio of the cross-polar to the co-polar signals. Assuming $\langle|s_{hv}|^2\rangle = \langle|s_{vh}|^2\rangle$ and $Z_{hv} = Z_{vh}$, the two possible measurements can be written in terms of scattering covariance elements as

$$LDR_{hv} = 10 \log(\langle|s_{hv}|^2\rangle/\langle|s_{vv}|^2\rangle)$$

and

$$LDR_{vh} = 10 \log(\langle|s_{hv}|^2\rangle/\langle|s_{hh}|^2\rangle)$$

or in terms of reflectivity as

$$LDR_{hv} = 10 \log (Z_{hv}/Z_v)$$

and

$$LDR_{vh} = 10 \log (Z_{hv}/Z_h) \quad .$$

LDR_{hv} and LDR_{vh} differ only by the differential reflectivity. Hence, they have similar properties.

The depolarized (cross-polar) signal stems from non-spheroidal particles which wobble as they fall, creating a distribution of canting angles, and from irregularly shaped particles. Signals are strongest for liquid or wetted particles because the refractive index for water is much greater than that for ice. The distribution of canting angles for raindrops is narrow–drops fall with their major axes close to the horizontal. Hence, LDR values for rain are small (on the order of -27 to -34 dB, Table 1). Values for dry snow are also small (< -25 dB) even if the particles wobble because their refractive index is small. LDR increases dramatically for wetted, tumbling particles with large axis ratios. Wet, melting snow has a LDR of > -18 dB. There is a wide category of partly wet snow in between dry and wet snow. Wet hail and graupel have a LDR of -10 to -25 dB. LDR is useful for detecting melting layers and hail.

As a ratio of reflectivities, LDR is insensitive to the absolute radar calibration and is independent of the drop concentration parameter N_0 (Table 2). Because the cross-polar power is two to three orders of magnitude smaller than the co-polar signal, the LDR measurement is susceptible to noise contamination, propagation effects, antenna misalignments, coupling between the two channels of the radar, and non-orthogonality of the electric vectors. For radars which make polarization measurements by switching between polarizations from pulse-to-pulse, LDR can be contaminated by second trip echoes. This property makes it attractive for detecting range folded echoes (Section 4.7.3). Scatter among individual LDR measurements along radials suggest the accuracy is 1 to 2 dB.

3.4 Correlation coefficient (ρ_{hv}) [2]

The co-polar correlation coefficient (ρ_{hv}) is computed from

$$\rho_{hv} = \langle s_{vv} s^*_{hh} \rangle / [\langle |s_{hh}|^2 \rangle^{1/2} \langle |s_{vv}|^2 \rangle^{1/2}]$$

and has both a magnitude and a phase (angle) given by the argument of $\langle s_{vv} s^*_{hh} \rangle$.[3] The magnitude, like the linear depolarization ratio, is sensitive to the dispersion in particle eccentricities, canting angles, irregular shapes, and the presence of mixed-phase precipitation. It is also influenced by backscatter phase shifts when Mie scatterers are present. Theoretical

[2]The notation for ρ_{hv} represents a special case, signifying that the parameter combines both co-polar returns.

[3]For radars transmitting alternate H and V polarizations, ρ_{hv} must be estimated. The technique is described by Balakrishnan and Zrnić (1990b).

values are ~0.99 for drizzle-sized drops and dry snow (Table 1). Slightly smaller coefficients exist for rain and ice crystals. Hall et al. (1980) found that $\rho_{hv} \gtrsim 0.98$ for rain. Mixed-phase precipitation characteristic of bright bands lowers the correlation because the variety of hydrometeor shapes and orientations increase. For hydrometeor distributions composed of melting snow, ρ_{hv} may be 0.8 to 0.95. The correlation coefficient can be as low as 0.80 for rain and hail mixtures. Thus, a possible use of ρ_{hv} is the detection of mixed-phase precipitation and hail. Compared to LDR, ρ_{hv} lacks capability to discriminate between light rain, dry snow, and graupel (Table 1).

Balakrishnan and Zrnić (1990b) assert that 128 sample pairs are needed to estimate ρ_{hv} with a precision of 0.01 (if the spectrum width is ≥ 4 m s^{-1}). Range averaging further reduces the error. Measured cross-correlation coefficients are influenced by system performance and polarization purity (Ryzhkov and Zrnić 1998b). Thus, thresholds given in Table 1 may vary from radar to radar. The correlation coefficient is sensitive to the signal-to-noise ratio and can be contaminated by sidelobes and ground clutter. The latter property can be useful for separating precipitation and ground echoes (Section 4.7.2).

The correlation coefficient is independent of N_0 and insensitive to hardware calibration (Table 2). There is, however, some sensitivity to the distribution of shapes. For example, based on simulations Balakrishnan and Zrnić (1990b) note that for a drop-size distribution composed only of 4-mm drops Z_{DR} is 2.5 dB and ρ_{hv} is 1.0. If the DSD contained drops of 2, 4, and 6-mm diameters in the proportion 200:1:0.01, Z_{DR} would be remain 2.5 dB but ρ_{hv} would be 0.988. In another example, they considered a distribution of infinitesimally thin cylinders and compared the ρ_{hv} signature with spheres. The correlation coefficient is 0.0 for the cylinders; and if half of the cylinders are oriented horizontally and half are oriented vertically, the differential reflectivity is 0 dB. For spherical particles Z_{DR} is 0 dB but ρ_{hv} is 1.0. Radar measurements reveal that the correlation coefficient is weakly related to differential reflectivity (Balakrishnan and Zrnić 1990b; Aydin and Giridhar 1992). As Z_{DR} increases, ρ_{hv} decreases slightly. For a distribution of raindrops ρ_{hv} should be relatively insensitive to small canting angles (Aydin and Giridhar 1992; Ryzhkov 2000).

3.5 Other backscattering measurements

The above quantities (Z_h, Z_v, Z_{DR}, LDR_{hv}, LDR_{vh}, and ρ_{hv}) use the 3 real diagonal terms and one complex off-diagonal term of the covariance matrix. The remaining covariance terms have been less studied. Ryzhkov (2000) and Ryzhkov et al. (2000a) investigated properties of the co-cross polar correlation coefficients at horizontal and vertical polarization (ρ_{xh} and ρ_{xv}) defined by

$$\rho_{xh} = \langle s_{hv} s^*_{hh} \rangle / [\langle |s_{hh}|^2 \rangle^{1/2} \langle |s_{hv}|^2 \rangle^{1/2}]$$

and

$$\rho_{xv} = \langle s_{hv} s^*_{vv} \rangle / [\langle |s_{vv}|^2 \rangle^{1/2} \langle |s_{hv}|^2 \rangle^{1/2}] \quad .$$

The magnitudes of these depolarization terms are sensitive to the angular distribution of scatterers, i.e., the mean canting angle and the dispersion about the mean. Mean canting angles for precipitation, when averaged over long transmission paths, are close to zero; but for individual measurement volumes they can be significantly nonzero. A range dependency in the magnitudes of ρ_{xh} and ρ_{xv} may be an indication of a radar problem such as feed horn misalignment or non-orthogonal electric vectors. The correlations can be used to detect non-Rayleigh (Mie) scatterers such as hail and large, wet snowflakes and may be useful for signaling the onset of electrification in storms.

That leaves three terms in the backscattering covariance matrix whose properties are yet to be discussed. The term $\langle s_{hh} s^*_{vv} \rangle$ can be used to form a correlation coefficient with properties that should be similar to ρ_{hv} except for a change in phase. Similarly, the remaining terms, $\langle s_{hh} s^*_{hv} \rangle$ and $\langle s_{vv} s^*_{hv} \rangle$, are not strictly independent but related to their symmetrical counterparts $\langle s_{hv} s^*_{hh} \rangle$ and $\langle s_{hv} s^*_{vv} \rangle$ by phase angles.

3.6 Differential propagation phase (ϕ_{DP}) and specific differential phase (K_{DP})

The above polarimetric parameters are derived from power measurements that depend upon the backscattering properties of illuminated particles. Radar waves are also subject to propagation effects such as attenuation and phase shifts. In an anisotropic medium like rain or pristine ice crystals, propagation constants for horizontally and vertically polarized waves differ. Horizontally polarized waves "see" a larger particle cross section and consequently propagate more slowly than vertically polarized waves. Backscattered signals return to the receiver with different accumulative phase (time) shifts depending on the hydrometeor size, shape, orientation, quantity, distance from the radar, and polarization state. The differential phase (ϕ_{DP}) is computed from

$$\phi_{DP} = \phi_{hh} - \phi_{vv}$$

where ϕ_{hh} and ϕ_{vv} are the two-way phase angles (in degrees) of the radar signals at horizontal and vertical polarization at a particular range location.

A more useful parameter is the specific differential phase (K_{DP}), defined as one half the range derivative of the two-way differential phase, i.e.,

$$K_{DP} = 0.5 \, \Delta\phi_{DP} / \Delta r$$

where Δr is the range increment over which $\Delta\phi_{DP}$ is measured. The units of K_{DP} are ^{o} km^{-1}. The specific differential phase can be computed from the DSD with (Oguchi 1983)

$$K_{DP} = \frac{180}{\pi}\lambda Re \int_0^{D_{max}} [f_{hh}(D) - f_{vv}(D)]N(D)\,dD$$

where Re refers to the real part of the integral, and f_{hh} and f_{vv} are the forward-scattering amplitudes for horizontally and vertically polarized waves.

The differential phase shift ϕ_{DP} actually has two components, a propagative component related to the difference in forward-scattering amplitudes and a component related to a backscatter differential phase. The total differential phase is

$$\phi_{DP} = 2\int_0^r K_{DP}\,dr + \delta$$

where the backscatter differential phase (δ, in deg) in the absence of propagation is given by

$$\delta = \arg(\langle s_{vv} s^*_{hh} \rangle)$$

and arg is the argument between s_{vv} and s^*_{hh}. The backscatter differential phase becomes significant when Mie scatterers (e.g., melting aggregates and hail) are present (e.g., Zrnić et al. 1993, Ryzhkov and Zrnić (1994), Kennedy et al. 1995). Zrnić and Ryzhkov (1998) show how the backscatter differential phase when combined with differential reflectivity can help discriminate between radar returns from insects and birds. For rain δ should be small at S-band.

The speed at which an electromagnetic wave propagates through a hydrometeor is inversely proportional to the refractive index. Hence, the differential phase is sensitive to the water content of the medium (see, e.g., Fig. 1). K_{DP} is insensitive to the isotropic constituents of mixed-phase precipitation.

The standard deviation of the ϕ_{DP} measurement is influenced by the co-polar correlation coefficient and the Doppler spectrum width. Sachidananda and Zrnić (1987) determined that for 128 horizontal and vertical pulse pairs the standard measurement error in ϕ_{DP} is $< 1.72^\circ$ when the spectrum width is > 1 m s^{-1} and the correlation coefficient is > 0.98. Ryzhkov and Zrnić (1996) found the standard error to be 2° in stratiform rain and $3-4^\circ$ in convection.

To reduce the error in estimates of K_{DP}, the ϕ_{DP} measurements are filtered in range (Hubbert et al. 1993; Aydin et al. 1995; and Ryzhkov and Zrnić, 1996). Estimates of K_{DP} accuracy vary. Balakrishnan and Zrnić (1990a), estimate errors can be as large as $\pm 0.7^\circ$ km^{-1}. Liu et al. (1993) and Aydin et al. (1995) estimate the error to be ± 0.25 and $\pm 0.50^\circ$ km^{-1}, respectively. From an analysis of 15 storms Ryzhkov and Zrnić (1996) determined a standard error in K_{DP} of 0.04 to 0.10° km^{-1} for a heavily-filtered version of their algorithm and an error between 0.12 and 0.30° km^{-1} for a lightly-filtered version. Errors on the order of 0.25° km^{-1} and larger would have pronounced effects on estimated rainfalls (Section 4.2.4).

The specific differential phase has a number of useful properties. It is insensitive to

radar calibration, part beam blockage, propagation effects, and system noise (Table 2). Potential uses of K_{DP} include the estimation of moderate and heavy rain rates (Section 4.2.4), correction for attenuation losses (Section 4.7.4), and verification of radar hardware calibration (Section 4.7.1). Because K_{DP} is insensitive to isotropic scatterers, it can be used to discriminate non-spherical particles from spherical or tumbling forms and to compute the fractional contribution of rain to total reflectivity in a rain/hail mixture (Section 4.4).

While it may be easier to make phase measurements than amplitude (power) measurements, there are some potential problems. Sachidananda and Zrnić (1987) note that the phase of radar signals is more readily contaminated by sidelobe signals than is the power measurement. Such errors may be manifest as high ϕ_{DP} in regions of low Z_h. Sachidananda and Zrnić estimate that sidelobe returns must be down more than 18 dB from main beam signals to ensure that bias errors are $< 0.5^o$. Another problem, particularly for quantitative rainfall estimation is that of negative K_{DP}s (Section 4.2.4). Negative values arise from statistical errors in the ϕ_{DP} measurement, from side lobes, clutter, range folded echoes, non-Rayleigh scatterers, and non-uniform distributions of precipitation. The latter issue is discussed by Ryzhkov and Zrnić (1996 and 1998a) and by Gorgucci et al. (1999b). A possible correction scheme, based on the expected consistency between specific differential phase computed from radar reflectivity and differential reflectivity and that observed, is described by Gorgucci et al. Genuine negative K_{DP} signals arise when electrical fields cause ice particles to be aligned with their principal axes in the vertical.

3.7 Difference reflectivity (Z_{DP})

A parameter useful for studying rain/ice mixtures is the difference reflectivity (Golestani et al. 1989)

$$Z_{DP} = 10 \log(Z_h - Z_v)$$

where $Z_h > Z_v$. This parameter is similar to differential reflectivity (a ratio, Section 3.2) and can be used to detect hail (Section 4.3.3) and to compute the fractional contribution of raindrops and ice to the total reflectivity in mixed-phase precipitation (Section 4.4). Caveats regarding clutter and sidelobe contamination apply. The parameter is sensitive to radar calibration error and responds to DSD variations. The scatter among point measurements suggests an accuracy of 1-2 dB.

4. POTENTIAL APPLICATIONS

4.1 Computation of drop-size distribution parameters

The degree of raindrop flattening is determined by the drop's size and is quantified by

the ratio of its minor and major axes (Section 1). Jameson (1983) determined that raindrop axis ratios for a monodispersed DSD are related to differential reflectivity (linear units) by $Z_{DR} = (a/b)^{-7/3}$. An axis ratio of 0.6 associates with a Z_{DR} of 3.29 (5.1 dB). Ulbrich and Atlas (1984) derived relations between the median volume diameter D_0 and Z_{DR} in the form

$$Z_{DR} = \alpha D_0^{1.55}$$

where $\alpha = 0.764$ dB mm$^{-1.55}$ for an exponential drop distribution and $\alpha = 0.580$ dB mm$^{-1.55}$ for a gamma DSD with $\mu = 2$. The slope parameter Λ can be computed from D_0 and the shape parameter μ with $\Lambda=(3.67+\mu)/D_0$ (Ulbrich 1983). Following Doviak and Zrnić (1993), N_0 can be computed from

$$N_0 = \frac{Z_h}{(6+\mu)!}\Lambda^{7+\mu} \quad [mm^{-(1+\mu)}\ m^{-3}] \quad .$$

Thus, if μ is known, assumed, or the DSD is exponential, the parameters Λ and N_0 can be determined from Z_{DR} and Z_h. [In theory, with another independent parameter (e.g., ρ_{hv}) a three parameter DSD (N_0, Λ, and μ) could be calculated.] Balakrishnan and Zrnić (1990b) show that ρ_{hv} and Z_{DR} are related weakly through μ (their Fig. 1a). As μ decreases, the correlation coefficient decreases, particularly for $Z_{DR} \gtrsim 2$ dB. Thus, it may be possible to find a value of μ from Z_{DR} and ρ_{hv} measurements that is consistent with their simulations. Additional measurements introduce new errors. Determination of a three or four parameter DSD is appropriate only if the added terms (μ or D_{max}) are a major source of error.

A study in which N_0 and D_0 were computed from radar measurements was conducted by Hall et al. (1980). They found that N_0 varied from 1×10^2 to 3×10^6 mm^{-1} m^{-3}, differing from the Marshall-Palmer value of 8000 mm^{-1} m^{-3} by more than a factor of 300. Their data reveal D_0 variations between 1 and 2.5 mm. In a similar study Bringi et al. (1998) estimate that D_0 was measured with a bias of 0.07 mm and a standard deviation of 0.35 mm.

Comparisons between radar measurements and raindrop disdrometer observations disclose a curious result. When Goddard and Cherry (1984) compared Z_{DR} values computed from disdrometer measurements using the equilibrium shapes of Pruppacher and Beard (1970) with radar measurements, they found that disdrometer-based Z_{DR}s exceeded radar measurements by 0.1 dB. They suggest that the drops were more spherical than that given by equilibrium shapes. [In the free atmosphere collisions between drops and/or turbulence could cause drop oscillations (canting) and further reduce Z_{DR}.] The DSD measurements of Goddard and Cherry were made with an impact disdrometer. This instrument is known to underestimate the number of smaller drops (Tokay and Short 1996, Tokay et al. 1999). However, the Goddard and Cherry finding seems supported by Chandrasekar et al. (1988) and Bringi et al. (1998) who compared radar measurements and DSD observations from aircraft. A recent laboratory wind tunnel experiment (Andsager et al. 1999) also seems to confirm the radar-based studies. Resolution of drop shape and canting issues has importance

for rainfall estimation.

4.2 Rainfall estimation

4.2.1 BACKGROUND

If the drop spectra [N(D)] is known, the rainfall rate (R) can be computed from

$$R = 6\pi \times 10^{-4} \int_0^{D_{max}} D^3 v_t(D) N(D) dD \quad [mm\ h^{-1}] \quad (3)$$

where $v_t(D)$ is the drop terminal velocity. Several relationships for v_t appear in the literature. Atlas et al. (1973) derived

$$v_t = 9.65 - 10.3 \exp(-6D) \quad [m\ s^{-1}] \quad (4)$$

where D is in cm. A simpler form is that of Atlas and Ulbrich (1977)

$$v_t = 17.67 D^{0.67} \quad [m\ s^{-1}] \quad . \quad (5)$$

Substituting Eqs. 1 and 4 into Eq. 3 (with an upper dropsize limit of infinity) yields (Doviak and Zrnić 1993)

$$R = 3.6 x 10^6 \frac{\pi N_0}{\Lambda^4} \left[9.65 - \frac{10.3}{(1 + 0.6/\Lambda)^4}\right] \quad .$$

Note that this expression is a two parameter estimate of the rainfall rate. A three parameter expression for rain rate (N_0, Λ, and μ) can be derived by substituting Eq. 2 into Eq. 3.

Factors that contribute to rainfall estimate errors are listed in Table 3. Although polarimetric measurements provide additional information regarding DSD variations, are relatively insensitive to hardware calibration, and provide information on precipitation phase, important error sources remain. Also, polarimetric rainfall estimation studies cited in the sections which follow have focussed on radar-gauge comparisons at short radar distances. The utility of the polarimetric rainfall estimates at long range has not been determined.

4.2.2 RADAR REFLECTIVITY

To estimate the rainfall rate with Eq. 3 it is necessary to know N(D). For an

exponential drop-size distribution (Eq. 1) this requires knowing N_o and Λ. Unfortunately, radars with a single polarization state measure only one useful parameter, Z_h, which combines the effects of N_o and Λ. Marshall and Palmer (1948) reduced the unknowns by assuming that N_o was constant. But subsequent study (Section 1) has shown that N_o can vary greatly. Raindrop disdrometer measurements disclose that N_o and Λ are only weakly related. Consequently, unique relationships between radar reflectivity and rainfall rate do not exist. Therefore, radar meteorologists have sought to establish empirical relationships of the form $Z=\alpha R^{\beta}$. Battan (1973) lists 69 different relations found by investigators. A well-known relationship attributed to Marshall and Palmer is

$$Z_h = 200R^{1.6} \quad (6)$$

where Z_h is in $mm^6\ m^{-3}$ and the rain rate R is in $mm\ h^{-1}$.[4] The default radar reflectivity estimator [$\Re(Z_h)$] used on the WSR-88D is

$$Z_h = 300R^{1.4} \quad . \quad (7)$$

Problems inherent in rainfall estimation with radar reflectivity are well known (Table 3). Z-R relations are sensitive to drop-size fluctuations, and rain rates can vary considerably for a given radar reflectivity. Wilson and Brandes (1979) show that mean storm-to-storm bias factors can easily vary by more than a factor of two even though a radar may be well calibrated climatologically (see also Steiner et al. 1999, Brandes et al. 1999, and Klazura et al. 1999). Bias factors show considerable variation even when storms are stratified by storm type (Klazura et al. 1999).

4.2.3 DIFFERENTIAL REFLECTIVITY

The potential of improving rainfall estimates with the differential reflectivity measurement was first discussed by Seliga and Bringi (1976, 1978). They showed how the ratio of Z_h and Z_v, represented by Z_{DR} (Section 3.2), is sensitive to the flattening of raindrops and could be used to estimate rain rate. The problem was cast in terms of N_0 and D_0 (i.e., for an exponential DSD) as

$$R = 0.6\times10^{-3}\pi N_0 \int_0^{D_{max}} D^3 v_t \exp(-3.67D/D_0)\,dD \quad .$$

D_0 and N_0 were estimated from Z_{DR} and Z_h. Seliga et al. (1981) applied the method to a single rain event. A mean bias of 1.02 was found for the differential reflectivity-based rainfall rate estimator [$\Re(Z_{DR})$]. Radar reflectivity estimators gave bias errors of 1.33 and 0.66.

---

[4] Marshall and Palmer (1948) actually determined $Z=220R^{1.6}$ which was later modified by Marshall et al. (1955).

The fractional standard error was 16% for the $\Re(Z_{DR})$ estimator and averaged 19% for the two radar reflectivity estimators used by Seliga et al. [Rain accumulation and rate errors for various polarimetric estimators are summarized in Table 4.]

The utility of differential reflectivity for improving rainfall estimates was also examined by Ulbrich and Atlas (1984). From simulations they derived

$$R = 1.93 \times 10^{-3} Z_h Z_{DR}^{-1.5}$$

for an exponential DSD and

$$R = 1.70 \times 10^{-3} Z_h Z_{DR}^{-1.5}$$

for a gamma distribution with $\mu = 2$. The units are $mm^6 m^{-3}$ for Z_h and dB for Z_{DR}. [Several candidate $\Re(Z_{DR})$ estimators found by various investigators are listed in Table 5.] Note that this form is valid for $Z_{DR} > 0$ dB. Application would require that negative values be reset to some positive value or that the rain rate be computed with another estimator. It is clear with these expressions that Z_{DR} is a modifier for Z_h. When raindrops are relatively small (large) as indicated by small (large) Z_{DR}, rain rates for a given radar reflectivity are adjusted upward (downward). Ulbrich and Atlas determined that compared to radar reflectivity alone their $\Re(Z_{DR})$ estimator reduced errors in rainfall rate by a factor of two. The maximum error reduction (33 to 14%) was for the gamma DSD.

Sachidananda and Zrnić (1987) derived a $\Re(Z_{DR})$ estimator from simulations in which the governing parameters for the exponential distribution (Eq. 1) and the maximum allowable drop size (D_{max}) for rainfall rate integration of Eq. 3 were allowed to vary randomly according to

$$\begin{aligned} 30 \geq N_o \geq 30{,}000 \quad & [mm^{-1} m^{-3}] \\ 1.0 \geq \Lambda \geq 4.5 \quad & [mm^{-1}] \\ 4.0 \geq D_{max} \geq 6.0 \quad . \quad & [mm] \end{aligned}$$

Equilibrium axis ratios were computed from the relationship of Green (1975, Section 1), and particle terminal velocities were taken from Eq. 5. The derived rainfall estimator was

$$R = 6.84 \times 10^{0.1(Z_h - 30 - 4.86 Z_{DR})} \quad . \quad (8)$$

Units are dBZ for reflectivity and dB for differential reflectivity. Sachidananda and Zrnić found that the standard errors with Eq. 8 due to DSD variability are ~15% at a rain rate of 50 mm h^{-1}. [Errors with a Marshall-Palmer DSD reflectivity estimator were 30%.]

A capability to respond to changes in drop size is a distinct advantage of differential reflectivity-based estimators. Compared to radar reflectivity, error reductions of a factor of 2 or more are possible (Table 4). Rain rate estimators (Table 5) for a given reflectivity and differential reflectivity measurement pair can differ substantially because of the different

models used (exponential versus gamma) and the expected range of the governing DSD parameters. The distribution of parameters in the free atmosphere is probably not random but more likely to be Gaussian. Parameters undoubtedly also vary from region-to-region, from season-to-season, and by storm type. Consequently, operational application will probably require some fine tuning for particular geographical regions.

Simulations suggest that derived relations are not overly sensitive to changes in D_{max}. The reason is that an increase (decrease) in D_{max} causes a corresponding increase (decrease) in both Z_h and Z_{DR}. The net effect on rainfall rate is small. Errors due to drop canting and assumed axis ratios are on the order of 5 to 10% (Aydin and Giridhar 1992). Rainfall rate estimates derived from differential reflectivity are susceptible to measurement errors especially at low Z_{DR}. Sachidananda and Zrnić (1987) caution that Z_{DR} must be measured to within 0.1 dB and Z_h to within 1 dB for acceptable rainfall rates. With Eq. 8 an error of 1 dB in radar reflectivity associates with an error in R of ~25%; an error of 0.1 dB in Z_{DR} associates with a R error of ~10%.

Chandrasekar and Bringi (1988) conclude that $\Re(Z_{DR})$ estimators do not out perform reflectivity at rainfall rates $\lesssim$ 20 mm h^{-1} because the error in the Z_{DR} measurement at low rain rates dominates over the information gathered concerning drop size. Jameson (1991) asserts that to achieve the full potential of the reflectivity/differential reflectivity parameter pair requires that Z_h be measured to an accuracy of at least 0.5 dB and Z_{DR} to better than 0.1 dB. Although spatial averaging will reduce measurement error, there will be a corresponding reduction in spatial resolution. Besides measurement error, Z_{DR}-based rainfall estimates are subject to ground clutter and sidelobe contamination. A potential serious problem for rainfall estimation is the presence of hail. Tumbling hail associates with high radar reflectivity and low differential reflectivity. Rain rates derived with hail-contaminated measurements can become astronomical. Fortunately, hail is readily detectable; and rainfall estimates can be made with other variables.

4.2.4 SPECIFIC DIFFERENTIAL PHASE

Research indicates that the specific differential phase (K_{DP}, Section 3.6) has several advantages over radar reflectivity (Z_h) for estimating rainfall (Ryzhkov and Zrnić 1995a,b; Zrnić and Ryzhkov 1996; Ryzhkov et al. 1997; Vivekanandan et al. 1999a). The signal arises from the retardation of radar waves whose polarization coincides with the principal axis of illuminated hydrometeors relative to an orthogonal wave. Because differential phase (ϕ_{DP}) is not a power measurement, rainfall estimates derived from K_{DP} are not susceptible to radar receiver or transmitter calibration error, attenuation, wet radomes, and beam blockage and are less affected by anomalous propagation. Rainfall rates from $\Re(K_{DP})$ estimators are also less sensitive than $\Re(Z_h)$ estimators to drop-size distribution variations (Sachidananda and Zrnić 1987) and to the presence of dry, tumbling hail (Balakrishnan and Zrnić 1990a, Aydin et al. 1995). The K_{DP} parameter is little affected by ground-clutter cancelers (Zrnić and Ryzhkov 1996).

Ryzhkov and Zrnić (1996) show that for intense rainfalls (generally characterized by drops with large median volume diameters) K_{DP} is related to the 4.24th power of the drop-size distribution (DSD), and for light rainfall rates K_{DP} is related to the 5.6th power of the DSD. Hence, K_{DP} is more closely related to rainfall rate (a 3.67th moment of the DSD) than is radar reflectivity (a 6th moment). The benefit is greatest at the higher rainfall rates.

Sachidananda and Zrnić (1987) performed simulations with the Marshall-Palmer DSD and derived a relationship between rain rate and K_{DP}. N_o was set at 8,000 mm^{-1} m^{-3}; D_{max} and Λ were varied randomly over the ranges

$$1.0 \geq \Lambda \geq 4.5 \qquad [mm^{-1}]$$
$$4.0 \geq D_{max} \geq 6.0 \qquad [mm] \quad .$$

The derived relationship was

$$R = 40.56\, K_{DP}^{0.866} \qquad (9)$$

where K_{DP} has the units ^{o} km^{-1}.

A simulation with gamma DSDs by Chandrasekar et al. (1990), with the following parameter limits

$$10^{4.2}\exp(2.8\mu) \leq N_0 \leq 10^{5.5}\exp(3.57\mu) \qquad [m^{-3}\ m^{-1-\mu}]$$
$$0 < D_0 \leq 2.5 \qquad [mm]$$
$$-1 < \mu \leq 4$$
$$D_{max} = 8 \qquad [mm]$$

produced the $\Re(K_{DP})$ estimator

$$R = 40.5\, K_{DP}^{0.85} \quad .$$

Other relations have been derived by Jameson (1991) and Aydin and Giridhar (1992) (Table 6). Rates for the various estimators differ by $\lesssim$ 10% over much of the expected range for significant rainfalls. The fact that all derived relationships are very similar supports the notion that $\Re(K_{DP})$ estimators are relatively insensitive to DSD variations.

Sachidananda and Zrnić (1987) found that the standard error with Eq. 9 at a rainfall rate of 50 mm h^{-1} due to DSD variations was less than 15%. Corresponding errors for the $\Re(Z_h)$ and $\Re(Z_{DR})$ estimators were 30 and 15% (Table 4). Ryzhkov and Zrnić (1995a) found that DSD-related errors with Eq. 9 were 60 to 80% larger than with the $\Re(Z_{DR})$ estimator (Eq. 8) but much smaller than those derived from radar reflectivity (their Table 1). When the likely impact of measurement errors was considered, the $\Re(K_{DP})$ estimator had the smaller error. At a rainfall rate of 100 mm h^{-1} the error was a factor of 4 less.

Simulations show that $\Re(K_{DP})$ estimators are not sensitive to variations in D_{max}. There is, however, a sensitivity to assumed axis ratios. Sachidananda and Zrnić (1987) conducted

an experiment in which the axis ratios were allowed to vary and found that rain rates changed by 18%. Chandrasekar et al. (1990) found rain rate differences of 30 to 50% between experimentally determined and equilibrium axis ratios. Drop canting causes small rainfall rate underestimates (~6%, Aydin and Giridhar 1992). Considering all issues, Chandrasekar et al. (1990) recommend that $\Re(K_{DP})$ estimators be applied to heavy rainfalls ($R > 70$ mm h^{-1}). Radar measurements presented by Ryzhkov and Zrnić (1996, their Fig. 6) indicate that the K_{DP} signal is significant for radar reflectivities $\gtrsim$ 40 dBZ (roughly a rainfall rate of 12 mm h^{-1}).

Radar-based computations of K_{DP} often yield negative values. Phase measurements have a significant standard error which is reduced by filtering (Section 3.6). Negatives of a statistical nature may remain after filtering. Other possible sources of negative values are side lobes, ground targets, and range folded echoes. Negatives occasionally detected in thunderstorm anvils are thought to associate with vertically aligned ice crystals in the presence of electrical fields (Caylor and Chandrasekar 1996). Large wet aggregates and hail can also have a significant backscatter differential phase that causes negative K_{DP} (Balakrishnan and Zrnić 1990b). Non-uniform distributions of precipitation can result in both positively and negatively biased K_{DP} (Ryzhkov and Zrnić 1998a, Gorgucci et al. 1999b).

Ryzhkov and Zrnić assert that to avoid bias due to statistical errors at low rain rates it is necessary to incorporate both the positive and negative values of K_{DP} in rainfall computations. Consequently, they suggest using estimators of the form

$$R = \mathrm{sign}(K_{DP})\, 40.56\, |K_{DP}|^{0.866} \quad . \quad (10)$$

Gorgucci et al. (1999b) propose a correction scheme for K_{DP} based on the expected consistency among K_{DP}, Z_h, and Z_{DR} measurements. The method has not been tested for rainfall estimation.

$\Re(K_{DP})$ estimators have been evaluated in several studies. For a single storm and 42 gauge-radar comparisons, Ryzhkov and Zrnić (1995a) determined that the RMSE for the $\Re(K_{DP})$ estimator (Eq. 9) was 28%. The errors for a radar reflectivity estimator (Eq. 6) and a differential reflectivity-based estimator (Eq. 8) were 31 and 38%, respectively. A comparison involving 15 storms was presented by Ryzhkov and Zrnić (1996). After excluding an outlier event dominated by small drop sizes, they determined a fractional standard error for Eq. 10 of 14%. The error was 38% for radar reflectivity. The improvement came from a reduction in the mean bias and in the scatter among bias factors for individual storms. Brandes et al. (2000) found that $\Re(Z_h)$ and $\Re(K_{DP})$ rainfall estimators were roughly equivalent for a well-calibrated radar. Correlation coefficients between radar-derived estimates from K_{DP} and raingauge observations were slightly lower than those from Z_h. This was attributed to the smoothing performed to compute K_{DP} and uncompensated negative K_{DP}s. The consistency between the two estimators was regarded as important for establishing the credibility of the estimated rainfalls. In the Ryzhkov and Zrnić (1996) and Brandes et al. (2000) studies the rainfall was underestimated by ~10%. Ryzhkov et al. (2000a) suggest this result could arise from a dispersion in the mean canting angle of 10 to 15°. Another

possibility is that the bias is introduced by the filtering of ϕ_{DP} (Gorgucci et al. 1999). Of the studies with $\Re(K_{DP})$ estimators summarized in Table 4 an improvement over radar reflectivity is evident in 4 of the 5 studies. Less certain is the utility of K_{DP} compared to $\Re(Z_{DR})$ estimators.

Because K_{DP} is a radial derivative of the total differential phase, the integrated rainfall over a particular range interval is given approximately by the ϕ_{DP} values at the end points of the interval. Watershed rainfalls estimated from boundary values of ϕ_{DP} should be less susceptible to ϕ_{DP} measurement error and to biases that result from nonuniform distributions of precipitation. Ryzhkov et al. (2000b) applied the boundary technique to a watershed having dimensions of a few tens of kilometers and compared results to rainfalls derived from the distribution of K_{DP} within the watershed. The boundary method had a bias of -8.2% compared to -12.7% for the standard method. Fractional standard errors were reduced from 25 to 18%. Computational requirements for the proposed method are reduced because the rainfall estimates are based on the measured ϕ_{DP} and not the computed K_{DP}.

4.2.5 Other combinations of polarimetric variables

To reduce the errors in rainfall rates that arise from DSD variations, Jameson (1991) used simulations to derive a $\Re(Z_{DR}, K_{DP})$ estimator

$$R = 6.242\ K_{DP}^{0.975}[1 - Z_{DR}^{-3/7}]^{-0.975}$$

where Z_{DR} has linear units. In a similar study, Ryzhkov and Zrnić (1995a) derived

$$R = 57.4\ K_{DP}^{0.935}\ Z_{DR}^{-0.704}$$

for light rainfall rates and

$$R = 52.0\ K_{DP}^{0.96}\ Z_{DR}^{-0.447}$$

for $R \geq 20$ mm h^{-1}. The standard errors due to DSD variations with the latter relation ranged from 1.1 to 3.1 mm h^{-1} over the rainfall rate interval of 10 to 200 mm h^{-1}. In a radar-gauge evaluation, which included the Jameson relation, Ryzhkov and Zrnić show for a single storm that $\Re(Z_{DR}, K_{DP})$ estimators produce rainfall estimates with a slightly smaller RMSE than with K_{DP} alone. The RMSE was a factor of 1.5 to 2 lower than that for $\Re(Z_H)$ and $\Re(Z_{DR})$ estimators. Jameson and Ryzhkov and Zrnić caution that measurement uncertainty will in general prevent the high accuracy implied by simulations.

Because the differential reflectivity and specific phase parameters have different properties and strengths, a possible procedure may be to use each rainfall estimator over its optimum range. Chandrasekar et al. (1990) suggest the following ranges of applicability

$\Re(Z_H)$ $R \leq 20$ mm h^{-1}
$\Re(Z_{DR})$ $20 < R < 70$ mm h^{-1}
$\Re(K_{DP})$ ≥ 70 mm h^{-1} .

While elements of this approach are embodied in a number of studies discussed here, a vigorous evaluation of such a procedure has not been made.

4.3 Hail detection

In this section polarimetric hail signatures and prospects for hail detection algorithms are discussed. While detection schemes based just on radar reflectivity and differential reflectivity are likely to be successful, the redundancy represented by the ensemble of measurements may be useful for eliminating false alarms. The ideal hail detection algorithm may incorporate a fuzzy logic weighing of variables.

Estimates of hail size and rates are highly desired but difficult to retrieve. The problem is complicated by the need to know the distributions of shape, orientation, and hail composition. Also, the relationship between Z_H and hail size becomes ambiguous at larger hailstone sizes. Attempts at hail rate modeling and size determination are not treated explicitly in this report. Readers are referred to studies by Ulbrich and Atlas (1982), Bringi et al. (1986), Balakrishnan and Zrnić (1990a,b), and Husson and Pointin (1989). Polarimetric measurements show considerable promise for hail detection, but a definitive study comparing polarimetric methods with reflectivity-based techniques has not been done.

4.3.1 Differential reflectivity

Harper (1962) first suggested that the difference in backscatter cross sections at horizontal and vertical polarization could be used to detect hail. This notion was explored by Seliga and Bringi (1978) who modeled hail as oblate spheroids with their major axes in the horizontal. They found that as large hail increased in size Z_{DR} decreased–eventually to negative values at a diameter of ~5 cm. The signature arises simply from size considerations. As hailstone diameters enter the Mie scattering range, a resonance occurs between hailstone size and reflectivity (see Fig. 8.4 of Battan 1973). For an oblate hailstone the reflectivity at vertical polarization can be higher than that at horizontal polarization even though the major axis of the hailstone lies in the horizontal plane. Wetting enhances the effect.

Differential reflectivity measurements imply that hail does not fall with a preferential alignment but tumbles creating a distribution of near random orientations. Thus, detection is predicated largely on signature differences for random (isotropic) and aligned (anisotropic) hydrometeor orientations. The principal axes of raindrops are nearly horizontal, $Z_h > Z_v$, and Z_h and Z_{DR} are positively correlated. Hail, graupel, and aggregates tend to tumble and fall with random orientation. Radar reflectivity of hail is typically > 50 dBZ (Table 1) because of

the 6th power dependency on particle diameter. Tumbling reduces Z_{DR} to 1 dB or less. Within hail shafts Z_h and Z_{DR} are negatively correlated. Although hail is readily distinguished from rain with Z_{DR}, separation from other ice forms is more difficult.

The potential of differential reflectivity for discriminating between rain and hail was demonstrated by Bringi et al. (1984). Rain was distinguished by low to moderate radar reflectivity ($\lesssim$45 dBZ) and Z_{DR} as large as 4 dB. Hail was characterized by radar reflectivity > 55 dBZ and Z_{DR} values near 0 dB. Strong Z_{DR} gradients delimited hail shafts. In Fig. 1 a hail shaft, manifest by a differential reflectivity minimum, exists at a range of 50 km.

With large hail it is frequently observed that Z_{DR} is < 0 dB (e.g., Lipschutz et al. 1986; Bringi et al. 1984; Zrnić et al. 1993; Ryzhkov and Zrnić 1994; Kennedy et al. 1995). As noted above, this result can arise simply because the hail is large. However, large hail may be less spherical than small hail and may fall with its major axis aligned vertically (Knight and Knight 1970) causing Z_{DR} to be negative. Balakrishnan and Zrnić (1990b) show that Z_{DR} could be less than -1 dB for wet or spongy hail with axis ratios > 0.7 if the major axes are close to vertical.

An "operational" evaluation of differential reflectivity for hail detection was conducted by Lipschutz et al. (1986). The approach was based on the work of Leitao and Watson (1984) who found that radar reflectivity and differential reflectivity measurement pairs were grouped and suggested that measurements well outside the rain envelope would signify the presence of ice forms. An experimental hail detection algorithm, based on polarimetric measurements, had a probability of detection (POD) of 0.56 compared to a radar reflectivity-based algorithm (the original NEXRAD algorithm) of 0.68. Lipschutz et al. note that many of polarimetric algorithm failures were for small hail and attributed the problem to imposed parameter thresholds. In spite of the disappointing results, they conclude that the polarimetric technique had great potential but needed further testing.

4.3.2 Differential reflectivity hail signal

To detect hail Aydin et al. (1986) proposed the differential reflectivity hail signal H_{DR} defined as

$$H_{DR} = Z_h - f(Z_{DR}) \quad [\text{dB}]$$

where

$$\begin{aligned} f(Z_{DR}) &= 27 \text{ dB} && Z_{DR} \le 0 \text{ dB} \\ &= 27 \text{ dB} + 19 \times Z_{DR} && 0 \le Z_{DR} \le 1.74 \text{ dB} \\ &= 60 \text{ dB} && Z_{DR} > 1.74 \text{ dB} \quad . \end{aligned}$$

H_{DR} weighs the departure of a particular Z_h observation from the rain/hail boundary $f(Z_{DR})$ in Z_h and Z_{DR} space. The boundary is based on simulated radar data from disdrometer

measurements in "rain-only" storms. Positive departures ($H_{DR} > 0$ dB) signify hail. The approach is another adaptation of that described by Leitao and Watson (1984).

An example of the distribution of radar reflectivity factor and differential reflectivity measurements in a hail storm is presented in Fig. 2. The segmented line represents the function $f(Z_{DR})$ and is intended to separate "rain-only" from "mixed-phase" (hail-contaminated) measurements. The departure of a particular observation from the line is H_{DR}. Although there is considerable scatter in the measurements, two dominant regimes can be seen. Measurements clustered along a curved line from Z_h = 20 dBZ, Z_{DR} = 0.4 dB to Z_h = 40 dBZ, Z_{DR} = 1.6 dB to Z_h = 55 dBZ, Z_{DR} = 3.6 dB, represent rain. Data points distributed roughly from Z_h =55 dBZ, Z_{DR} = 3.0 dB to Z_h 67 dBZ, Z_{DR} = 0.4 dB signify hail-contaminated measurements.

In Fig. 2 the actual boundary between rain and hail-contaminated measurements is made diffuse by mixtures of rain and hail, e.g., near 55 dBZ and Z_{DR} = 3.0 dB. Also, meteorological conditions can alter DSDs and consequently relationships between Z_h and Z_{DR}. For rain consisting of relatively small drops, the distribution of points in Fig. 2 would be shifted downward which could trigger hail designations. A more powerful hail-detection parameter may be the gradient of H_{DR}.

There is some evidence that H_{DR} can be used to quantify hailstone size. For a limited dataset Brandes and Vivekanandan (1998) show that H_{DR} increases with hail size. The correlation between maximum hail diameter and H_{DR} was 0.65; the correlation between maximum hail diameter and radar reflectivity was 0.33. The lower correlation with reflectivity was attributed to the resonance between hail and the radar wavelength for diameters in the Mie scattering range.

4.3.3 Difference reflectivity

Golestani et al. (1989) propose to detect hail with the difference reflectivity

$$Z_{DP} = 10 \log(Z_h - Z_v) \quad [\text{dB}]$$

where $Z_h > Z_v$. Again, the procedure is to determine departures from the rain-only case. An example of the radar reflectivity-difference reflectivity distribution in a hail storm is shown in Fig. 3. The scatter is due in part to statistical error in the measurements and to variations in the DSD. The sloped line gives the relationship between Z_h and Z_{DP} for rain-only measurements and was determined by applying a least-squares fit to those measurements unlikely to be contaminated by hail ($H_{DR} < -5$ dB). Alternately, the analysis could be performed on storms known not to have produced hail. The equation for the line is

$$Z_{DP} = -11.6 + 1.17\, Z_h \quad . \quad (11)$$

Ice is signified by measurements that depart significantly to the right of the line. The ice

signature begins approximately at a reflectivity of 55 dBZ. Small departures probably indicate small ice cores within large raindrops. Large departures for radar reflectivities > 55 dBZ are hail contaminated.

A disadvantage of Z_{DP} for hail designation is that the parameter is undefined for $Z_h < Z_v$. Thus, special designations would have to be made for those mixed-phase data points seen in Fig. 2 with radar reflectivities of ~60 dBZ and negative differential reflectivities. Relationships between Z_{DP} and Z_h for rain, like those for Z_{DR} and Z_h, are sensitive to DSD variations. At a given reflectivity, a Z_{DP} observation above the rain line associates with more flattened (larger) drops, and observations which fall below the line associate with more spherical (smaller) drops. An important property of Z_{DP} is that it allows the estimation of the ice contribution to radar reflectivity and thereby potentially improving rainfall estimates in mixed-phase precipitation (Section 4.4).

4.3.4 Specific differential phase

Inconsistencies between Z_h and K_{DP} can indicate hail. K_{DP} is sensitive to anisotropic hydrometeors such as rain and pristine ice crystals; dry, tumbling hail with a completely random distribution of orientations has no signature. For the Marshall-Palmer drop-size distribution, Balakrishnan and Zrnić (1990a) derived the relationship

$$Z = 13.86 \log(K_{DP}) + 44 \quad [\text{dBZ}]$$

where Z is the average of reflectivities at horizontal and vertical polarization. This relation "predicts" that a K_{DP} of 4° km^{-1} associates with a Z_h of 52 dBZ. An observed reflectivity greater than 52 dBZ would indicate the presence of hail. For radar measurements in rain Balakrishnan and Zrnić also determined that

$$Z = 8 \log(K_{DP}) + 49 \quad [\text{dBZ}]$$

(their Fig. 1). They point out that the two Z-K_{DP} relations intersect at 56 dBZ which is close to the WSR-88D default threshold of 55 dBZ for hail.

As indicated in Table 1, K_{DP} signatures for hail are generally not 0° km^{-1} but can vary over a wide range. Radar signals from large hail may have a backscatter phase shift (Zrnić et al. 1993, Ryzhkov and Zrnić (1994), Kennedy et al. 1995) indicated by large spatial variations in ϕ_{DP} and possibly negative K_{DP}. On the other hand, the formation of a horizontal torus of liquid about melting hail could cause large positive values of K_{DP}.

4.3.5 Correlation coefficient and linear depolarization ratio

The correlation coefficient ρ_{hv} is sensitive to particle canting angles, irregular shapes,

differential phase shifts for Mie scatterers, particle eccentricities, and ensembles of ice and liquid-phase hydrometeors. Balakrishnan and Zrnić (1990b) use simulations and observations to show that the correlation coefficient is > 0.98 for pure rain. However, for wet or spongy hail and for hail with large protuberances, ρ_{hv} falls below 0.95. Occasionally, radar measurements of ρ_{hv} in severe hail storms are < 0.80 (e.g., Fig. 1, at a range of 52 km and a height of 5 km; Ryzhkov and Zrnić 1994). Such hail is probably large with a significant backscatter phase shift.

The linear depolarization ratio, being sensitive to canting angles and irregular shapes, also responds to hail. Signatures for large wet hail can be as large as -10 dB (Table 1). In Fig. 1 LDR > -13 dB is indicated at a range of 52 km and a height of 6 km. Importantly, hail signatures for LDR and ρ_{hv} often persist well above the melting layer and remain distinguishable from other ice forms such as dry and dense snow.

4.4 Estimating rainfall when hail is present

A method whereby the contribution of raindrops to reflectivity in a rain-hail mixture can be computed is described by Golestani et al. (1989). For rain there is a linear relationship between Z_{DP} and Z_h (e.g., Fig. 3). If ice particles tumble and have no preferred orientation or if they are spherical in shape, their contribution to reflectivity at horizontal and vertical polarization is the same, i.e., $Z_{h,ice} = Z_{v,ice}$. The implication is that ice makes no contribution to Z_{DP}. Hence, the relation between Z_{DP} and Z_h (Eq. 11, Section 4.3.3) can be written

$$Z_{h,rain} = (Z_{DP} + 11.6)/1.17 \quad [\text{dBZ}]$$

and can be used to compute $Z_{h,rain}$ when hail is present . The fraction of rain (f) is

$$f = Z_{h,rain}/(Z_{h,rain} + Z_{h,ice}) = Z_{h,rain}/Z_h \quad .$$

Use of $Z_{h,rain}$ rather than the hail-contaminated Z_h value should improve rainfall estimates with Z-R relations.

K_{DP} may also be used to find the rain contribution to Z_h when dry, tumbling hail is present. Under these conditions the specific differential phase rainfall estimator $\Re(K_{DP})$ is sensitive only to the rain portion of the medium. Thus, the rainfall rate could be estimated from K_{DP}. The rain rate could then be substituted into a Z_h–R relation to find the rain contribution to Z_h. Application of this method requires that both rain rate estimators [$\Re(K_{DP})$ and $\Re(Z_h)$] be unbiased. The inferred rain contribution to reflectivity could be compared to that computed independently from the difference reflectivity (Z_{DP}).

4.5 Bright bands

Dry snow and dense snow consisting of pristine ice crystals are usually characterized by relatively low Z_h (Table 1) due to their low refractive index. The differential reflectivity can be as large as 5 dB for dense anisotropic ice crystals but is usually small (< 1 dB) for low-density irregular ice particles (also Vivekanandan et al. 1994). When particles begin to melt, they appear to radar as water droplets of equivalent size. Battan (1973) has shown this behavior begins if only 10% of an ice particle melts. The reflectivity of the mixed-phase particle increases by 6.7 dB due simply to the change in refractive index. This increase is offset somewhat by the reduction in particle size which accompanies melting and an increase in terminal velocity which evacuates particles from the radar volume. Melting effects on radar reflectivity are readily detected in stratiform precipitation but are often suppressed in strong convection (e.g., Fig. 1).

Examples of polarimetric signatures for the melting layer in the declining stratiform rain region of a mesoscale convective system are shown in Fig. 4. Vertical profiles of mean radar reflectivity, differential reflectivity, linear depolarization, and correlation coefficient are presented. [Other examples can be found in Bader et al. 1987; Illingworth and Caylor 1989; Hall et al. 1984; Frost et al. 1991; and Herzegh and Jameson 1992.] The radar reflectivity increase toward ground actually begins well above the 0°C level (4.6 km, dashed line). The initial enhancement is likely due to greater stickiness of the ice particles at relatively warm but still sub-freezing temperatures—a process called sintering. The maximum reflectivity, slightly below the 0°C level, represents the combined effects of aggregation, melting, and changes in terminal velocity.

Examination of the polarimetric parameters in Fig. 4 shows a Z_{DR} maximum (bright band) of 1.1 dB. [The minimum just above the 0°C level is believed to be an artifact created by mismatches between the horizontal and vertical beams of the radar.] The lower level of the Z_{DR} maximum compared to the reflectivity maximum suggests that maximum eccentricity (flatness) of the particles occurs at a lower level than their maximum size. The vertical distribution of Z_{DR} clearly shows two precipitation regimes, an upper layer of ice particles with Z_{DR} of ~0.2 dB and a lower layer of rain with Z_{DR} close to 1 dB. Similar distributions are seen in convective storms as well (Figs. 1 and 5).

The presence of mixed-phase precipitation types in the melting layer reduces ρ_{hv} to < 0.93. The signal is likely enhanced by the wobbling of large aggregates, some of which may enter the Mie scattering range, and by a broadening of the hydrometeor distribution of shapes and sizes. Linear depolarization ratio (LDR) measurements in the melting layer increase to a maximum of -16 dB. The correlation coefficient and linear depolarization often show melting layer signatures when they are not evident in radar reflectivity and differential reflectivity measurements.

Polarimetric measurements should permit the determination of freezing levels in nearly all precipitating systems. When signatures are absent, e.g., with strong convection, it should be possible to estimate freezing levels from measurements in adjacent areas. Knowing that sub-freezing temperatures exist below a bright band is strong evidence that freezing rain may be occurring. A refreezing of the droplets in the sub-freezing layer would initiate tumbling which would be detectable with the Z_{DR} measurement.

Melting layer effects are readily detected in vertical cross sections because of the sharp contrasts in polarimetric signatures for dry snow, wet snow, and rain layers and the short distances over which they occur. An important but more difficult application is the operational discrimination between rain and snow with radar measurements made at constant elevation angle. Ryzhkov and Zrnić (1998c) found that under these conditions a sharp ρ_{HV} minimum marked the boundary between snow and rain when large snowflakes existed in the transition zone. In other situations the transition was characterized by an increase in Z_{DR}.

4.6 Hydrometeor discrimination

Because polarimetric measurements are sensitive to particle size, shape, orientation, phase (liquid or solid), and density (wet, dry, aggregates, or rimed), particular hydrometeor types have characteristic signatures. The ensemble of measurements and derived parameters (e.g., standard deviations of radial velocity, differential reflectivity, and differential phase) can be used to designate the dominant scatterers within the radar volume. In this section proposed schemes for general hydrometeor classification are reviewed. The methods incorporate experiences gained from a multitude of studies involving simulations and observations. Polarimetric signatures for specific hydrometeors are not always unique; and in general, bulk rather than detailed information can be obtained. Nevertheless, there is great potential for detecting weather hazards (rain-snow boundaries, hail, freezing rain, and icing conditions), for cloud microphysical studies, and for improving precipitation parameterization in numerical models.

Hall et al. (1980) first discussed how dual-polarization measurements could be used for hydrometeor discrimination. They argued that, unless ice particles have large asymmetries, Z_{DR} would be small due to a low refractive index. Compact ice particles (graupel) should also have small Z_{DR}. Similarly, they deduced characteristic signatures for rain, drizzle, dry snowflakes, wet snow, wet graupel, wet hail, and dry hail. In a heuristic study, Hall et al. (1984) outlined a rule-based technique for hydrometeor discrimination that incorporated reflectivity and differential reflectivity (their Fig. 4). Expected ranges of Z_{DR} and general characterizations of radar reflectivity (low, medium, and high) for various hydrometeor types were given. They used the standard deviation of differential reflectivity to detected ground clutter.

A summary of characteristic polarimetric radar signatures (Z_h, Z_{DR}, ρ_{hv}, K_{DP}, and LDR) for drizzle, rain, and various snow, graupel, and hail categories useful for hydrometeor classification has been given by Doviak and Zrnić (1993) (their Table 8.1, reproduced here as Table 1). A hydrometeor discrimination algorithm, based in large part on the parameter values given by Doviak and Zrnić, was proposed by Straka and Zrnić (1993). Höller et al. (1993) present similar classifications (at C-band) and applied a prototype hydrometeor discrimination algorithm to a hail storm. The controlling parameters were Z_{DR} and LDR. Classification types included small and large drop rainfalls; dry small graupel and snow; small wet graupel, large graupel, and small dry hail; dry hail; wet hail; large hail; and rain-hail

mixtures. Their thresholds differ slightly from those of Doviak and Zrnić. Exactly how the final classifications were obtained when conflicts arose is not discussed. An example of hydrometeor designations in a hail storm was presented by Zrnić et al. (1993).

The precipitation-typing study of López and Aubagnac (1997) is based on Z_h, Z_{DR}, and K_{DP}. Thresholds for rain, dry and wet graupel, small and large hail, and rain/hail mixtures are mostly taken from Doviak and Zrnić (1993). Conflicts among particle types were resolved with a rule-based system. An adaptation of the relationships found by Balakrishnan and Zrnić (1990a) between radar reflectivity and specific phase was used to distinguish pure rain from mixed-phase precipitation. Another rule assumed that the precipitation was frozen if K_{DP} was less than 0.5° km^{-1} and Z_h was greater than 40 dBZ. The technique was successfully applied to a hail storm.

It is clear from Table 1 and the classification parameter thresholds of Hall et al. (1984) and Höller et al. (1993) that signatures for many particle types are not unique but overlap. This prompted the development of a "fuzzy-logic" approach to particle discrimination by Vivekanandan et al. (1999b). The proposed methodology employs "membership functions" to determine the degree to which a particular radar parameter (radar reflectivity, differential reflectivity, ... etc.) belongs to a particular type classification (rain, hail, wet snow, ...). The shape of the membership function for each radar measurable is based on knowledge gained from observational studies and simulations appearing in the literature. Function output is a number "P" which varies from 0 to 1 denoting the membership amount in the particular class. For example, hail because of its large size associates with high radar reflectivity. The membership function for radar reflectivity in hail classification assigns P a value of 0 for a reflectivity value < 45 dBZ. The value of P increases linearly from 0 to 1 as reflectivity increases from 45 to 50 dBZ. Reflectivity values greater than 50 dBZ are assigned a value of 1. The P values for each radar parameter are weighed and summed. The final algorithm classification is the precipitation category with the largest accumulated value. The fuzzy logic approach ensures that particular classifications are insensitive to the details of the membership functions. The precise shape of the membership functions and the weights of each measurement can be tuned and adjusted for different storm types and geographical regions.

The algorithm described by Vivekanandan et al. (1999) attempts to make 17 different classifications. An example is given in Fig. 5. Liquid and frozen precipitation zones are clearly shown. Designated ice forms include irregular ice crystals, dry snow, and graupel/small hail categories. A wet snow layer marks the melting layer. Although signatures for rain, hail, wet snow, and insects are well established by numerous observational studies, a capability to designate other echo types (e.g., cloud drops, drizzle, supercooled liquid water, irregular ice crystals, dry crystals, dry versus wet hail) are less certain and more difficult to verify.

Because polarimetric variables with the exception of K_{DP} are derived from power measurements, hydrometeor designations will generally apply to the larger and/or wetted particles within the radar volume and may not be representative of the most numerous particle type. Side lobe, mismatched beam patterns, and low signal-to-noise ratio impacts on the performance of potential algorithms have not been thoroughly investigated. Herzegh and

Carbone (1984) show examples of large positive Z_{DR} signatures that arise through sidelobes. The issue was further explored by Liu and Herzegh (1986) who found that large positive and presumably biased Z_{DR} is often associated with reflectivity gradients. In Fig. 4 the slightly negative Z_{DR} at the top of a radar reflectivity bright band is thought to have been created by mismatches in mean beam shapes in the presence of strong vertical gradients of reflectivity.

Few studies have sought to verify radar-based hydrometeor designations with in situ cloud observations. Bader et al. (1987) determined that the designation of individual particle types from in situ measurements was not always possible because many particles, particularly larger ones, were not always well formed; and the presence of large irregular particles and aggregates tended to mask radar signatures from smaller aligned crystal forms (see also Liu and Herzegh 1986). Bader et al. and Liu and Herzegh note that although ice particles can fall with a preferred orientation their low bulk density and refractive index will often result in small Z_{DR} signatures and make discrimination from other hydrometeor types difficult.

4.7 Data quality assessment

4.7.1 System calibration

Measurements of Z_h, Z_{DR}, and K_{DP} are closely related and constrained by meteorological factors. In the absence of non-meteorological contamination, the consistency among parameters can be exploited for hardware self-calibration (Goddard et al. 1994). Scarchilli et al. (1996) derived an expression for estimating specific phase (K_{DP}^*) from Z_h and Z_{DR} in the form

$$K^*_{DP} = 1.05\times10^{-4}\, Z_h^{0.96}\, 10^{-0.26 Z_{DR}}$$

where Z_h has the units $mm^{-6}\ m^{-3}$ and Z_{DR} is in dB. Differences between estimated and radar-measured K_{DP} are an indication of calibration error. The method is further discussed by Gorgucci et al. (1999a) who stress the need to correct the radar reflectivity and differential reflectivity measurements for attenuation losses (Section 4.7.4) before applying the technique. Consistency checks are thought to improve the overall radar calibration to $\pm$ 0.5 dB. Gorgucci et al. (1999b) determined that non-uniform distributions of precipitation result in biased values of K_{DP} derived from measurements of ϕ_{DP}. This bias must be considered when using K_{DP} to determine system calibration error and would seem to limit calibration checks to precipitation regions with little gradient.

Range trends in LDR and the co-cross-polar correlation coefficients ρ_{xh} and ρ_{xv} are possible indicators of misalignments in the antenna feed horn and non-orthogonality between horizontal and vertical radar beams. Thus, such checks can be important for evaluating system purity.

4.7.2 ANOMALOUS PROPAGATION/GROUND CLUTTER/BEAM BLOCKAGE

Polarimetric measurements Z_{DR}, ρ_{hv}, LDR, and ϕ_{DP}, when contaminated by ground clutter, contrast sharply with signals from precipitation echoes. The multi-path returns from clutter behave much like noise and are characterized by large spatial fluctuations. Differential reflectivity measurements from ground clutter typically exhibit a broad range of values (± 4 dB and more) with standard deviations from data bin to data bin of ≥ 1 dB. Standard deviations for precipitation are usually < 0.5 dB. Correlation coefficients for single-phase precipitation are generally > 0.95, but in clutter regions ρ_{hv} rapidly falls below 0.95 and may be < 0.7. Standard deviations for ρ_{hv} are 0.02 in precipitation and > 0.1 for clutter. Differential propagation phase measurements from clutter are random and distributed over the interval ±180° and may have a standard deviation of 10° or more. Measurements from precipitation typically show standard deviations of 3 to 4°. Consequently, permanent ground clutter and anomalous propagation are readily discerned.

Ground clutter was detected with the standard deviation of differential reflectivity in the study of Hall et al. (1984). For rain with radar reflectivity between 15 and 40 dBZ the differential reflectivity varied from 0 to 1.2 dB. The standard deviations were 1 to 3 dB for reflectivity and < 0.13 dB for differential reflectivity. For ground clutter Z_{DR} ranged from -4.3 to +4.6 dB and had a standard deviation of 1.5 to 3.5 dB. The reflectivity characteristics of the clutter (local mean and standard deviation) were similar to that for the rain. In the study of Brandes et al. (1999) the standard deviation of differential reflectivity, computed for a five data bin running window, was used to identify ground echoes. Central data bins with a standard deviation of > 1 dB were considered to be contaminated by clutter. This simple clutter rejection scheme, when applied to a mixed AP and precipitation event, improved reflectivity rainfall estimates from a bias factor of 0.57 and a correlation between gauge and radar amounts of 0.65 to 0.93 and 0.91, respectively.

Rainfall estimates in storms with mixtures of precipitation and anomalous propagation echoes have been made by Ryzhkov and Zrnić (1998b). Ryzhkov and Zrnić determined that ground clutter was characterized by a ρ_{hv} of 0.4 to 0.7 and that in precipitation ρ_{hv} is greater than 0.8. They note, however, that a precise clutter threshold may vary somewhat for different radars because the ρ_{hv} measurement is affected by system performance and polarimetric purity. Nonetheless, the technique should work well for situations where precipitation echoes and AP are separated or precipitation echoes dominate. Complications may arise if hail or wet snow is present and ρ_{hv} falls below 0.8.

Ryzhkov and Zrnić (1998b) recommend a different procedure for situations in which clutter echoes are embedded within precipitation. The normal steady increase in ϕ_{DP} in precipitation may be masked in regions dominated by ground clutter. Stable trends in ϕ_{DP} resume if "good" precipitation echoes are again encountered at more distant ranges. Rainfall rates in regions dominated by ground clutter and AP can be estimated from ϕ_{DP} discontinuities between adjacent uncontaminated precipitation zones. Ryzhkov and Zrnić applied their method to a mixed precipitation and AP event where echo types were largely isolated. Watershed mean rainfalls were estimated with radar reflectivity and specific differential phase.

The mean rainfall for a 1 h period, as determined from gauges, was 5.2 mm. K_{DP} mean rainfall estimates for two filtering lengths were 4.7 and 4.8 mm. The reflectivity estimate, contaminated by clutter,was 6.6 mm.

Brandes et al. (2000) also show the benefit of the specific phase measurement in situations of mixed precipitation and AP echoes. Unedited rainfall estimates from radar reflectivity when compared to raingauge observations revealed a bias factor of 0.57 (nearly a factor of two overestimate). The correlation coefficient between the estimates and gauge observations was 0.65. Estimated rainfall accumulations from K_{DP} with no special editing had a much improved bias factor of 0.90 and a correlation with gauge observations of 0.87.

Beam blockage effects on rainfall estimates from radar reflectivity and specific phase measurements were studied by Zrnić and Ryzhkov (1996), who compared rainfall estimates for antenna elevation angles of 0 and 0.5°. Large differences in radar reflectivity rainfall estimates occurred for the two elevation angles. Root mean square errors where 6.89 and 3.01 mm, respectively. The large error at the lower elevation was attributed to beam blockage. In contrast, the RMSEs at 0 and 0.5° elevation for a combination of K_{DP} and Z_h parameters were 3.45 and 2.58 mm. This result seems to confirm that K_{DP}-derived rainfall estimates are insensitive to beam blockage. Also, the phase measurements can be made closer to the ground which should improve the correlation between gauge and radar-estimated rainfalls and reduce errors introduced by vertical gradients of precipitation.

Beam blockage effects for a flash flood event in mountainous terrain were investigated by Vivekanandan et al. (1999a). In regions with little blockage differences between rainfall estimates derived from radar reflectivity and specific phase were normally distributed and had near zero mean. In a region of up to 70% blockage, rainfall estimate differences were skewed, and $\Re(Z_h)$ estimates were reduced relative to $\Re(K_{DP})$ estimates. The reduction in rainfall estimates with $\Re(Z_h)$ was nearly linearly related to the percent blockage.

4.7.3 RANGE FOLDED ECHOES

Polarization radars making the linear depolarization ratio measurement typically operate by alternating the polarization of transmitted pulses and then sampling both the co-polar and cross-polar returns. Signals from second trip echoes will result in the $\langle |s_{vh}|^2 \rangle$ term in the LDR measurement (Section 3.3) being co-polar. Contaminated measurements are strong (often -10 to +20 dB) compared to first trip precipitation echoes (-34 to -10 dB). Contamination may occur even though the second trip echoes have negligible impact on radar reflectivity. The LDR increase below 1 km in Fig. 4 is an example.

4.7.4 ATTENUATION CORRECTION

Attenuation losses at S-band can be surprisingly large in extreme rainfall events characteristic of flash floods. For example, Ryzhkov and Zrnić (1995b) describe a radially

oriented squall line with reflectivity losses on the order of 10 dB and a differential reflectivity bias of -3 dB. Smyth and Illingworth (1998) discuss an event with a differential reflectivity bias of -5 dB. Obviously, a correction scheme is needed if accurate rainfall estimates and reliable hail detections are to be made for such events. Simple attenuation correction schemes based on reflectivity measurements are known to be highly unstable (Bringi et al. 1990; Smyth and Illingworth 1998). An attractive alternative is presented by the differential propagation phase measurement. ϕ_{DP} is not affected by attenuation; and because the measurement responds to drop oblateness, it is sensitive to factors that cause attenuation differences at horizontal and vertical polarization.

Bringi et al. (1990) derived linear relationships between the specific phase and the attenuation at horizontal polarization (A_h) and between specific phase and the differential attenuation (A_{h-v}, defined as the difference A_h-A_v). Using simulations with gamma drop-size distributions at a temperature of 15°C, they determined

$$A_h = 0.016K_{DP}$$

and

$$A_{h-v} = 0.00367K_{DP} \quad .$$

Similar relations were derived for disdrometer measurements. An intense rainfall with $K_{DP} = 4$ ° km^{-1} (R=135 mm h^{-1}, Eq. 9) suggests attenuation losses of 0.064 dB km^{-1} for radar reflectivity and 0.015 dB km^{-1} for differential reflectivity. Although the corrections are small, the accumulated losses can be large as noted above.

Assuming a linear relationship between attenuation and K_{DP}, Ryzhkov and Zrnić (1995b) determined experimentally that

$$A_h = 0.040K_{DP}$$

and

$$A_{h-v} = 0.0088K_{DP} \quad .$$

These corrections are considerably larger than the theoretical estimates of Bringi et al. (1990) and those found by Jameson (1992). Ryzhkov and Zrnić attribute this result to the presence of "giant" drops possibly supported by ice cores. Rainfall estimates from corrected reflectivities and reflectivity measurements from a second, unattenuated radar closely agreed.

Smyth and Illingworth (1998) also investigate methods for correcting radar reflectivity with polarimetric data. In particular they examine a thunderstorm which produced gauge-measured rain rates in excess of 250 mm h^{-1}. A re-examination of the Bringi et al. study prompted the conclusion that the use of a simple linear attenuation correction is tantamount to assuming that D_0 is constant but allowing N_0 to vary. Smyth and Illingworth assert that the

maximum value of D_0 used by Bringi et al. (2.5 mm) is too small for heavy precipitation. For a maximum D_0 of 5 mm and a N_0 of 8000 m^{-3} mm^{-1}, they find an attenuation coefficient of ~0.034 dB deg^{-1} (computed from their Fig. 5) which is intermediate between that of Bringi et al. (1990) and Ryzhkov and Zrnić (1995b).

Smyth and Illingworth propose a correction technique based on Z_{DR} depressions behind intense echoes and the radial distribution of K_{DP}. If Z_{DR} in light rainfall at the rear of a storm is -2 dB, they reason that the total path differential attenuation (A_{h-v}) must be 2 dB. The differential attenuation at each data gate is determined by partitioning the total differential attenuation according to the distribution of K_{DP} along the radial. N_0 and D_0 are found for an exponential DSD or for a gamma DSD with a specified μ. The DSD parameters are used to compute the incremental attenuations A_h and A_{h-v}, and subsequently the corrected Z_h and Z_{DR}.

Simulations (Jameson 1992) indicate that corrections are inversely related to temperature and can vary by as much as 75% as temperatures increase from 0 to 20°C. The accuracy of corrections depends upon the DSD, ϕ_{DP} measurement error, temperature, and whether or not there is a significant backscatter differential phase shift due to non-Rayleigh scatterers. The attractiveness of the specific phase technique is that the corrections are bounded by the measured ϕ_{DP} or Z_{DR} deficit.

Correction techniques have had little testing. Zrnić and Ryzhkov (1996) applied the relationship of Ryzhkov and Zrnić (1995b) to a single event and lowered the RMSE for radar reflectivity rainfall estimates from 3.01 to 2.77 mm (their Table 1). In the Smyth and Illingworth (1998) study there was good agreement between the corrected rainfall estimate and the observed rainfall at a gauge recording extreme rain rates. Curiously, at a second raingauge with relatively light rainfall rates, the estimates were reduced after attenuation correction. Presumably, the increase in Z_{DR} effectively reduced the number of small drops and lowered the rain rate estimate.

5. SUMMARY AND RECOMMENDATIONS

This report identifies important potential benefits with radar polarimetry that include improved rainfall estimation, hail detection, designation of rain-snow boundaries and melting layers, and general hydrometeor classification. Polarimetric measurements should also enhance data quality through improved hardware calibration, detection of ground clutter and anomalous propagation, identification of range folded echoes, and discrimination of biological targets. As an active area of research, additional applications are likely to evolve.

While research results are positive, it is evident that much work must be done before a commitment to polarimetry can be made. The first steps are already being taken at the National Severe Storms Laboratory in the modification of a WSR-88D for polarimetric measurements. A committee of research experts, operational radar meteorologists, and program managers should be established to focus and coordinate future activities. Committee tasks should include the planning of an extended operational demonstration program, selecting prototype algorithms for testing, and overseeing their evaluation. It's likely that polarimetric

algorithms will require some tuning for different geographical regions. This need can be fulfilled by taking advantage of field campaigns conducted within the research community. Finally, incorporation and successful application of the polarimetric measurements will require a heightened level of expertise. Thus, education and training needs will also have to be addressed.

REFERENCES

Andsager, K., K. V. Beard, and N. F. Laird, 1999: Laboratory measurements of axis ratios for large drops. J. Atmos. Sci., **56,** 2673-2683.

Atlas D., 1953: Optical extinction by rainfall. J. Meteor., **10,** 486-488.

_____, R. C. Srivastava, and R. S. Sekhon, 1973: Doppler radar characteristics at vertical incidence. Rev. Geophys. Space Phys., **2,** 1-35.

_____, and C. W. Ulbrich, 1977: Path- and area-integrated rainfall measurement by microwave attenuation in the 1-3 cm band. J. Appl. Meteor., **16,** 1322-1331.

_____, _____, F. D. Marks Jr., E. Amitai, and C. R. Williams, 1999: Systematic variation of drop size and radar-rainfall variations. J. Geophys. Res., **104,** 6155-6169.

Aydin, K., V. N. Bringi, and L. Liu, 1995: Rain-rate estimation in the presence of hail using S-band specific differential phase and other radar parameters. J. Appl. Meteor., **34,** 404-410.

_____, and V. Giridhar, 1992: C-band dual-polarization radar observables in rain. J. Atmos. Oceanic Technol., **9,** 383-390.

_____, T. A. Seliga, and V. Balaji, 1986: Remote sensing of hail with a dual-linear polarization radar. J. Climate Appl. Meteor., **25**, 1475-1484.

Bader, M. J., S. A. Clough, and G. P. Cox, 1987: Aircraft and dual polarization radar observations of hydrometeors in light stratiform precipitation. Q. J. Roy. Meteor. Soc., **113,** 491-515.

Balakrishnan, N., and D. S. Zrnić, 1990a: Estimation of rain and hail rates in mixed-phase precipitation. J. Atmos. Sci., **47,** 565-583.

_____, and _____, 1990b: Use of polarization to characterize precipitation and discriminate large hail. J. Atmos. Sci., **47,** 1525-1540.

Battan, L. J., 1973: Radar Observation of the Atmosphere, University of Chicago Press, 324 pp.

Brandes, E. A., A. V. Ryzhkov, and D. S. Zrnić, 2000: An evaluation of radar rainfall estimates from specific differential phase. Submitted to J. Atmos. Oceanic Technol. (In

revision)

_____, and J. Vivekanandan, 1998: An exploratory study in hail detection with polarimetric radar. Preprint, 14th International Conf. on Interactive Information and Processing Systems for Meteorology, Oceanography, and Hydrology, Phoenix, Arizona, Amer. Meteor. Soc., 287-290.

_____, _____, and J. W. Wilson, 1999: A comparison of radar reflectivity estimates of rainfall from collocated radars. J. Atmos. Oceanic Technol., **16,** 1264-1272.

Bringi, V. N., V. Chandrasekar, N. Balakrishnan, and D. S. Zrnić, 1990: An examination of propagation effects in rainfall on radar measurements at microwave frequencies. J. Atmos. Oceanic Technol., **7,** 829-840..

_____, _____, and R. Xiao, 1998: Raindrop axis ratios and size distributions in Florida rainshafts: An assessment of multiparameter radar algorithms. IEEE Trans. Geosci. Remote Sensing, **36,** 703-715.

_____, and A. Hendry, 1990. Technology of polarization diversity radars for meteorology. Radar in Meteorology, D. Atlas, Ed., Amer. Meteor. Soc., 153-190.

_____, T. A. Seliga, and K. Aydin, 1984: Hail detection with a differential reflectivity radar. Science, **225,** 1145-1147.

_____, J. Vivekanandan, and J. D. Tuttle, 1986: Multiparameter radar measurements in Colorado convective storms. Part II: Hail detection studies. J. Atmos. Sci., **43,** 2564-2577.

Caylor, J., and V. Chandrasekar, 1996: Time-varying ice crystal orientation in thunderstorms observed with multiparameter radar. IEEE Trans. Geosci. Remote Sens., **34,** 847-858.

Chandrasekar, V., and V. N. Bringi, 1988: Error structure of multiparameter radar and surface measurements of rainfall. Part I: Differential reflectivity. J. Atmos. Oceanic Technol., **5,** 783-795.

_____ and _____, N. Balakrishnan, and D. S. Zrnić, 1990: Error structure of multiparameter radar and surface measurements of rainfall. Part III: Specific differential phase. J. Atmos. Oceanic Technol., **7,** 621-629.

_____, W. A. Cooper, and V. N. Bringi, 1988: Axis ratios and oscillations of raindrops. J. Atmos. Sci., **45,** 1323-1333.

Doviak, R. J., V. Bringi, A. Ryzhkov, A. Zahrai, and D. Zrnić, 2000: Considerations for polarimetric upgrades to operational WSR-88D radars. J. Atmos. Oceanic Technol. **17,** 257-278.

_____, and D. S. Zrnić, 1993: Doppler Radar and Weather Observations, Academic Press, 562 pp.

Frost, I. R., J. W. F. Goddard, and A. J. Illingworth, 1991: Hydrometeor identification using cross polar radar measurements and aircraft verification. Preprints, 25th International Conf. on Radar Meteorology, Paris, France, Amer. Meteor. Soc., 658-661.

Goddard, J. W. F., and S. M. Cherry, 1984: The ability of dual-polarization radar (copolar linear) to predict rainfall rate and microwave attenuation. Radio Sci., **19,** 201-208.

_____, J. Tan, and M. Thurai, 1994: Technique for calibration of meteorological radars using differential phase. Electron. Lett., **30,** 166-167.

Golestani, Y., V. Chandrasekar, and V. N. Bringi, 1989: Intercomparison of multiparameter radar measurements. Preprints, 24th Conf. on Radar Meteorology, Tallahassee, Florida, Amer. Meteor. Soc., 309-314.

Gorgucci, E., V. Chandrasekar, and G. Scarchilli, 1995: Radar and surface measurement of rainfall during CaPE: 26 July 1991 case study. J. Appl. Meteor. **34,** 1570-1577.

_____, G. Scarchilli, and V. Chandrasekar, 1994: A robust estimator of rainfall rate using differential reflectivity. J. Atmos. Oceanic Technol., **11,** 586-592.

_____, _____, and _____, 1999a: A procedure to calibrate multiparameter weather radar using properties of the rain medium. IEEE Trans. Geosci. Remote Sensing, **37,** 269-276.

_____, _____, and _____, 1999b: Specific differential phase estimation in the presence of nonuniform rainfall medium along the path. J. Atmos. Oceanic. Technol., **16,** 1690-1697.

Green, A. W., 1975: An approximation for the shapes of large raindrops. J. Appl. Meteor., **14,** 1578-1583.

Hall, M. P. M., S. M. Cherry, J. W. F. Goddard, and G. R. Kennedy, 1980: Rain drop sizes and rainfall rate measured by dual-polarization radar. Nature, **285,** 195-198.

_____, J. W. F. Goddard, and S. M. Cherry, 1984: Identification of hydrometeors and other

targets by dual-polarization radar. Radio Sci., **19,** 132-140.

Harper, W. G., 1962: Radar back scattering from oblate spheroids. Nubila, **1,** 60-72.

Herzegh, P. H., and R. E. Carbone, 1984: The influence of antenna illumination function characteristics on differential reflectivity measurements. Preprints, 22nd Conf. on Radar Meteorology, Zurich, Switzerland, Amer. Meteor. Soc., 281-286.

_____, A. R. Jameson, 1992: Observing precipitation through dual-polarization radar measurements. Bull. Amer. Meteor. Soc., **73,** 1365-1374.

Höller, H., V. N. Bringi, J. Hubbert, and P. F. Meischner, 1993: Particle discrimination in hailstorms. Preprints, 26th International Conf. on Radar Meteorology, Norman, Oklahoma, Amer. Meteor. Soc., 594-595.

Hubbert, J., V. Chandrasekar, V. N. Bringi, and P. Meischner, 1993: Processing and interpretation of coherent dual-polarized radar measurements. J. Atmos. Oceanic Technol., **10,** 155-164.

Husson, D., and Y. Pointin, 1989: Quantitative estimation of the hailfall intensity with a dual polarization radar and a hailpad network. Preprints, 24th Conf. on Radar Meteorology, Tallahassee, Florida, Amer. Meteor. Soc., 318-321.

Illingworth, A. J., and I. J. Caylor, 1989: Cross polar observations of the bright band. Preprints, 24th Conf. on Radar Meteorology, Tallahassee, Florida, Amer. Meteor. Soc., 323-327.

_____, and M. P. Johnson, 1999: The role of raindrop shape and size spectra in deriving rainfall rates using polarization radar. Preprints, 29th International Conf. on Radar Meteorology, Montreal, Quebec, Canada, Amer. Meteor. Soc., 301-304.

Jameson, A. R., 1983: Microphysical interpretation of multi-parameter radar measurements in rain. Part I: Interpretation of polarization measurements and estimation of raindrop shapes. J. Atmos. Sci., **40,** 1792-1802.

_____,1991: A comparison of microwave techniques for measuring rainfall. J. Appl. Meteor., **30,** 32-54.

_____, 1992: The effect of temperature on attenuation-correction schemes in rain using polarization propagation differential phase shift. J. Appl. Meteor., **31,** 1106-1118.

Kennedy, P. C., V. N. Bringi, S. Bolen, and S. A. Rutledge, 1995: An examination of dual

polarization signatures associated with confirmed occurrences of large hail. Preprints, 27th Conf. on Radar Meteorology, Vail, Colorado, Amer. Meteor. Soc., 41-43.

Klazura, G. E., J. M. Thomale, D. S. Kelly, and P. Jendroski, 1999: A comparison of NEXRAD WSR-88D radar estimates of rain accumulation with gauge measurements for high- and low-reflectivity horizontal gradient precipitation events. J. Atmos. Oceanic Technol., **16,** 1842-1850.

Knight, C. A., and N. C. Knight, 1970: The falling behavior of hailstones. J. Atmos. Sci., **27,** 672-681.

Leitao, M. J., and P. A. Watson, 1984: Application of dual linearly polarized radar data to prediction of microwave path attenuation at 10-30 GHz. Radio Sci., **19,** 209-221.

Lipschutz, R. C., J. F. Pratte, and J. R. Smart, 1986: An operational Z_{DR}-based precipitation type/intensity product. Preprints, 23th Conf. on Radar Meteorology, Snowmass, Colorado, Amer. Meteor. Soc., JP91-JP94.

Liu, J.-L., and P. H. Herzegh, 1986: Differential reflectivity signatures in ice-phase precipitation: Radar-aircraft comparisons. Preprints, 23rd Conf. on Radar Meteorology, Snowmass, Colorado, Amer. Meteor. Soc., 59-61.

Liu, L., V. N. Bringi, I. J. Caylor, and V. Chandrasekar, 1993: Intercomparison of multiparameter radar signatures from Florida storms. Preprints, 26th Int. Conf. on Radar Meteorology, Norman, Oklahoma, Amer. Meteor. Soc., 733-735.

López, R. E., and J.-P. Aubagnac, 1997: The lightning activity of a hailstorm as a function of changes in its microphysical characteristics inferred from polarimetric radar observations. J. Geophys. Res., **102,** 16,799-16,813.

Marshall, J. S., W. Hitschfield, and K. L. S. Gunn, 1955: Advances in radar weather. Advances in Geophys., **2,** 1-56.

_____, and W. M. Palmer, 1948: The distribution of raindrops with size. J. Meteor., **5,** 165-166.

Oguchi, T., 1983: Electromagnetic propagation and scattering in rain and other hydrometeors. Proc. IEEE, **71,** 1029-1078.

Pruppacher, H. R., and K. V. Beard, 1970: A wind tunnel investigation of the internal circulation and shape of water drops falling at terminal velocity in air. Quart. J. Roy. Meteor. Soc., **96,** 247-256.

Ryzhkov, A. V., 2000: Interpretation of polarimetric radar covariance matrix for meteorological scatterers. Theoretical analysis. Submittted to J. Atmos. Oceanic Technol.

_____, and D. S. Zrnić, 1994: Precipitation observed in Oklahoma mesoscale convective systems with a polarimetric radar. J. Appl. Meteor., **33,** 455-464.

_____, _____, 1995a: Comparison of dual-polarization radar estimators of rain. J. Atmos. Oceanic Technol., **12,** 249-256.

_____, and _____, 1995b: Precipitation and attenuation measurements at 10-cm wavelength. J. Appl. Meteor., **34,** 2121-2134.

_____, and _____, 1996: Assessment of rainfall measurement that uses specific differential phase. J. Appl. Meteor., **35,** 2080-2090.

_____, and _____, 1998a: Beamwidth effects on the differential phase measurements of rain. J. Atmos. Oceanic Technol., **15,** 624-634.

_____, and _____, 1998b: Polarimtric rainfall estimation in the presence of anomalous propagation. J. Atmos. Oceanic Technol., **15,** 1320-1330.

_____, and _____, 1998c: Discrimination between rain and snow with a polarimetric radar. J. Appl. Meteor., **37,** 1228-1240.

_____, _____, and D. Atlas, 1997: Polarimetrically tuned R(Z) relations and comparison of radar rainfall methods. J. Appl. Meteor., **36,** 340-349.

_____, and _____, and R. Fulton, 2000a: Areal rainfall estimates using differential phase. J. Appl. Meteor., **39,** 263-268.

_____, _____, J. Hubbert, V. N. Bringi, J. Vivekanandan, and E. A. Brandes, 2000b: Interpretation of polarimetric radar covariance matrix for meteorological scatterers. Data Analysis. Submitted to J. Atmos. Oceanic Technol.

Sachidananda, M., and D. S. Zrnić, 1987: Rain rate estimates from differential polarization measurements. J. Atmos. Oceanic Technol., **4,** 588-598.

Scarchilli, G., E. Gorgucci, V. Chandrasekar, and A. Dobaie, 1996: Self-consistency of polarization diversity measurement of rainfall. IEEE Trans. Geosci. Remote Sensing, **34,** 22-26.

Sekhon, R. S., and R. C. Srivastava, 1970: Snow size spectra and radar reflectivity. J. Atmos. Sci., **27,** 299-307.

Seliga, T. A., K. Aydin, and H. Direskeneli, 1986: Disdrometer measurements during an intense rainfall event in Central Illinois: Implications for differential reflectivity radar observations. J. Climate Appl. Meteor., **25,** 835-846.

_____, and V. N. Bringi, 1976: Potential use of radar differential reflectivity measurements at orthogonal polarizations for measuring precipitation. J. Appl. Meteor., **15,** 69-76.

_____, and _____ 1978: Differential reflectivity and differential phase shift: Applications in radar meteorology. Radio Sci., **13,** 271-275.

_____, _____ , and H. H. Al-Khatib, 1981: A preliminary study of comparative measurements of rainfall rate using the differential reflectivity radar technique and a raingage network. J. Appl. Meteor., **20,** 1362-1368.

Smyth, T. J., and A. J. Illingworth, 1998: Correction for attenuation of radar reflectivity using polarization data. Quart. J. Roy. Meteor. Soc., **124,** 2393-2415.

Steiner, M., J. A. Smith, S. J. Burges, C. V. Alonzo, and R. W. Darden, 1999: Effect of bias adjustment and rain gauge data quality control on radar rainfall estimation. Water Resources Res., **35,** 2487-2503.

Straka, J. M., and D. S. Zrnić, 1993: An algorithm to deduce hydrometeor types and contents from multi-parameter radar data. Preprints, 26th International Conf. on Radar Meteorology, Norman, Oklahoma, Amer. Meteor. Soc., 513-515.

Tokay, A., and D. A. Short, 1996: Evidence from tropical raindrop spectra of the origin of rain from stratiform versus convective clouds. J. Appl. Meteor., **35,** 355-371.

_____, O. Thiele, A. Kruger, and W. Krajewski, 1999: New measurements of drop size distribution and its impact on radar rainfall retrievals. Preprints, 29th International Conf. on Radar Meteorology, Montreal, Quebec, Canada, Amer. Meteor. Soc., 659-662.

Ulbrich, C. W., 1983: Natural variations in the analytical form of the raindrop size distribution. J. Climat Appl. Meteor., **22,** 1764-1775.

_____, and D. Atlas, 1982: Hail parameter relations: A comprehensive digest. J. Appl. Meteor., **21,** 22-43.

_____, and _____ 1984: Assessment of the contribution of differential polarization to improved rainfall measurements. Radio Sci., **19,** 49-57.

Vivekanandan, J., V. N. Bringi, M. Hagen, and P. Meischner, 1994: Polarimetric radar studies of atmospheric ice particles. IEEE Trans. Geosci. Remote Sensing, **32,** 1-10.

_____, D. N. Yates, and E. A. Brandes, 1999: The influence of terrain on rainfall estimates from radar reflectivity and specific propagation phase observations. J. Atmos. Oceanic Technol., **16,** 837-845.

_____, D. S. Zrnić, S. M. Ellis, R. Oye, A. V. Ryzhkov, and J. Straka, 1999: Cloud microphysics retrieval using S-band dual-polarization measurements. Bull. Amer. Meteor. Soc., **80,** 381-388.

Waldvogel, A., 1974: The N_0 jump of raindrop spectra. J. Atmos. Sci., **31**, 1067-1078.

Wilson, J. W., and E. A. Brandes, 1979: Radar measurement of rainfall—A summary. Bull. Amer. Meteor. Soc., **60,** 1048-1058.

Zrnić, D. S., 1991: Complete polarimetric and Doppler measurements with a single receiver radar. J. Atmos. Oceanic Technol., **8,** 159-165.

_____, V. N. Bringi, N. Balakrishnan, K. Aydin, V. Chandrasekar, and J. Hubbert, 1993: Polarimetric measurements in a severe hailstorm. Mon. Wea. Rev., **121,** 2223-2238.

_____, and A. Ryzhkov, 1996: Advantages of rain measurements using specific differential phase. J. Atmos. Oceanic Technol., **13,** 454-464.

_____, and _____, 1998: Observations of insects and birds with a polarimetric radar. IEEE Trans. Geosci. Remote Sens., **36,** 661-668.

_____, and _____, 1999: Polarimetry for weather surveillance radars. Bull. Amer. Meteor. Soc., **80,** 389-406.

List of Symbols and Acronyms

a	particle minor axis
A_h, A_v	attenuation at horizontal and vertical polarization
A_{h-v}	differential attenuation
AP	anomalous propagation
b	particle major axis
D	equivalent volume diameter
D_h, D_v	diameter in horizontal and vertical planes
D_0	median volume diameter
DSD	drop-size distribution
f	fractional contribution of rain to radar reflectivity
$\|K\|^2$	dielectric factor
K_{DP}	specific differential phase
LDR	linear depolarization ratio
m	complex index of refraction
$N(D)$	hydrometeor number concentration
N_0	DSD concentration parameter
r	radar range
R	rainfall rate
$\Re$	rainfall rate estimator
v_t	terminal velocity
Z_{DP}	difference reflectivity
Z_{DR}	differential reflectivity
Z_h, Z_v	radar reflectivity at horizontal and vertical polarization
δ	backscatter differential phase
Λ	drop-size distribution slope
μ	drop-size distribution shape parameter
ρ_{hv}	co-polar correlation coefficient
ρ_{xh}	co-cross correlation coefficient (horizontal polarization)
ρ_{xv}	co-cross correlation coefficient (vertical polarization)
ϕ_{DP}	differential phase

Table 1. Values of polarimetric variables for precipitation types (from Doviak and Zrnić 1993).

	Z_h (dBZ)	Z_{DR} (dB)	ρ_{hv}	K_{DP} (^{o} km^{-1})	LDR (dB)
Drizzle	< 25	0	>0.99	0	<-34
Rain	25 to 60	.5 to 4	>0.97	0 to 10	-27 to -34
Dry snow	< 35	0 to .5	>0.99	0 to 0.5	<-34
Dense snow	< 25	0 to 5	>0.95	0 to 1	-25 to -34
Wet snow	< 45	0 to 3	0.8 to 0.95	0 to 2	-13 to -18
Dry graupel	40 to 50	-0.5 to 1	>0.99	-0.5 to 0.5	< -30
Wet graupel	40 to 55	-0.5 to 3	>0.99	-0.5 to 2	-20 to -25
Wet hail (< 2 cm)	50 to 60	-0.5 to 0.5	>0.95	-0.5 to 0.5	<-20
Wet hail (> 2 cm)	55 to 70	<-0.5	>0.96	-1 to 1	-10 to -15
Rain/hail	50 to 70	-1 to 1	>0.90	0 to 10	-10 to -20

Table 2. Attributes of polarimetric variables (from Zrnić and Ryzhkov 1999).

	Attribute				
Variable	Independent of absolute radar calibration	Immune to propagation effects	Immune to noise bias	Used for quantitative estimation	Independent of concentration
Z_h	no	no	no	yes	no
Z_{DR}	yes	no	no	yes	yes
K_{DP}	yes	yes	yes	yes	no
ρ_{hv}	yes	yes	no	no	yes
δ	yes	no	yes	no	yes

LDR	yes	no	no	no	yes

Table 3. Sources of error in radar rainfall estimates.

1) Temporal and spatial variations in DSD's
2) Advection of precipitation below the radar beam
3) Attenuation by rain, hail, wet radomes, and atmospheric gases
4) Precipitation gradients within the radar beam
5) Bright bands
6) Evaporation
7) Beam blockage
8) Ground clutter contamination
9) Changes in hydrometeor phase
10) Particle size sorting by the horizontal and vertical wind
11) Integration of temporal rain rate samples
12) Sampling differences
13) Hardware calibration

Table 4. Comparison of rainfall estimator errors (%). Errors for polarimetric variables tend to decrease as the rain rate increases. Errors for radar reflectivity are sensitive to the particular Z-R relation selected. Results for simulations including measurement errors can vary considerably according to the model used.

Study	Source	$\Re(Z_h)$	$\Re(Z_{DR})$	$\Re(K_{DP})$
Seliga et al. (1981)	radar and gauges	19	16	-
Ulbrich and Atlas (1984)	simulation	33	14	-
Seliga et al. (1986)	disdrometer	16-44	4-8	-
Sachidananda and Zrnić (1987)	simulation	30	15	15
Jameson (1991)	simulation	40	16	45
Aydin and Giridar (1992)	disdrometer	17-38	3-10	6-29
Ryzhkov and Zrnić (1995a)	radar and gauges	31	38	28

Gorgucci et al. (1995)	radar and gauges	49-58	35	-
Ryzhkov and Zrnić (1996)	radar and gauges	38		14

Table 5. Summary of $\Re(Z_{DR})$ estimators. Units for Z_h are $mm^6\ m^{-3}$ for all studies except Sachidananda and Zrnić where the units are dBZ. Units for Z_{DR} are dB except for the Jameson study where they are linear. Rainfall rates (R) are in mm h^{-1}.

Study	Source	Relation	DSD/notes
Ulbrich and Atlas (1984)	simulation	$R = 1.93\times10^{-3} Z_h Z_{DR}^{-1.5}$	exponential
	simulation	$R = 1.70\times10^{-3} Z_h Z_{DR}^{-1.5}$	gamma, $\mu = 2$
Sachidananda and Zrnić (1987)	simulation	$R = 6.84\times10^{0.1(Z_h - 30 - 4.86 Z_{DR})}$	exponential
Chandrasekar and Bringi (1988)	simulation	$R = 2.397\times10^{-3} Z_h^{0.94} Z_{DR}^{-1.08}$	gamma
Jameson (1991)	simulation	$R = 9.797\times10^{-3} Z_h Z_{DR}^{-5.80}$	gamma
Gorgucci et al. (1994)	simulation	$R = 10.0\times10^{-3} Z_h^{0.92} 10^{-0.369 Z_{DR}}$	gamma
Seliga et al. (1986)	disdrometer	$R = 1.95\times10^{-3} Z_h Z_{DR}^{-1.04}$	$0.2 \le Z_{DR} \le 0.7$ dB
	disdrometer	$R = 1.59\times10^{-3} Z_h Z_{DR}^{-1.67}$	$0.7 \le Z_{DR} \le 2.6$ dB
Aydin and Giridhar (1992)	disdrometer	$R = 2.38\times10^{-3} Z_h^{0.943} Z_{DR}^{-1.23}$	

Table 6. Summary of $\Re(K_{DP})$ estimators. K_{DP} units are $^o\ km^{-1}$; R is in mm h^{-1}.

Study	Source	Relation	DSD
Sachidananda and Zrnić (1987)	simulation	$R = 40.56 K_{DP}^{0.866}$	Marshall-Palmer
Chandrasekar et al. (1990)	simulation	$R = 40.5 K_{DP}^{0.85}$	gamma
Jameson (1991)	simulation	$R = 41.46 K_{DP}^{0.838}$	gamma
Aydin and Giridar (1992)	disdrometer	$R = 36.15 K_{DP}^{0.84}$	gamma, $0.01 < K_{DP} < 1.5\ ^o\ km^{-1}$
	disdrometer	$R = 33.77 K_{DP}^{0.97}$	gamma, $1.5 \le K_{DP} < 7\ ^o\ km^{-1}$

List of Symbols and Acronyms

a	particle minor axis
A_h, A_v	attenuation at horizontal and vertical polarization
A_{h-v}	differential attenuation
AP	anomalous propagation
b	particle major axis
D	equivalent volume diameter
D_h, D_v	diameter in horizontal and vertical planes
D_0	median volume diameter
DSD	drop-size distribution
f	fractional contribution of rain to radar reflectivity
$\|K\|^2$	dielectric factor
K_{DP}	specific differential phase
LDR	linear depolarization ratio
m	complex index of refraction
$N(D)$	hydrometeor number concentration
N_0	DSD concentration parameter
r	radar range
R	rainfall rate
$\Re$	rainfall rate estimator
v_t	terminal velocity
Z_{DP}	difference reflectivity
Z_{DR}	differential reflectivity
Z_h, Z_v	radar reflectivity at horizontal and vertical polarization
δ	backscatter differential phase
Λ	drop-size distribution slope
μ	drop-size distribution shape parameter
ρ_{hv}	co-polar correlation coefficient
ρ_{xh}	co-cross correlation coefficient (horizontal polarization)
ρ_{xv}	co-cross correlation coefficient (vertical polarization)
ϕ_{DP}	differential phase

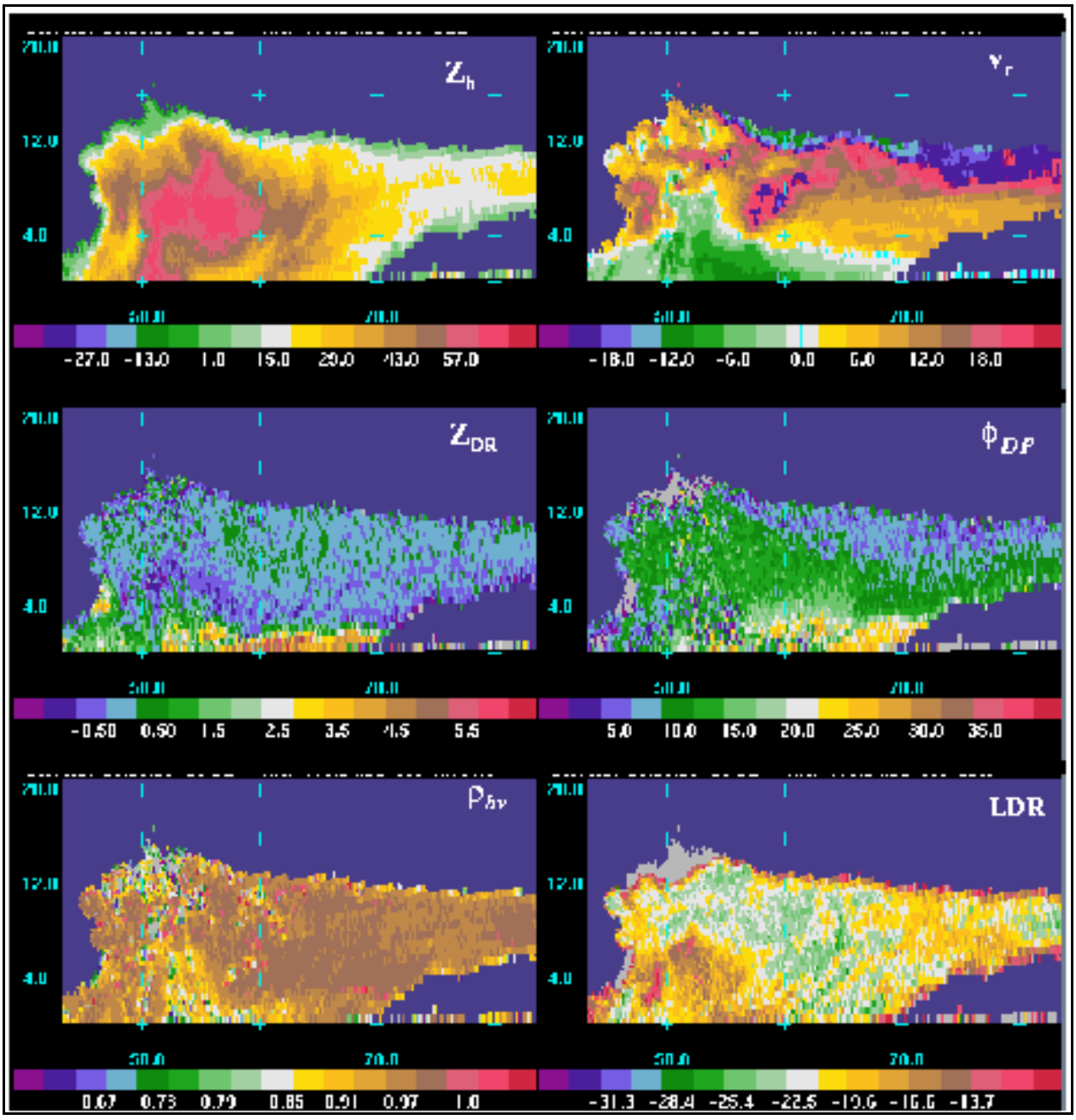

Fig. 1. Vertical cross section through a severe hail storm observed near Wichita, Kansas on 13 June 1997. Panels show radar reflectivity (Z_h), radial velocity (v_r), differential reflectivity (Z_{DR}), differential phase (ϕ_{DP}), correlation coefficient (ρ_{hv}), and linear depolarization ratio

(LDR). Distances (tick marks) are in kilometers.

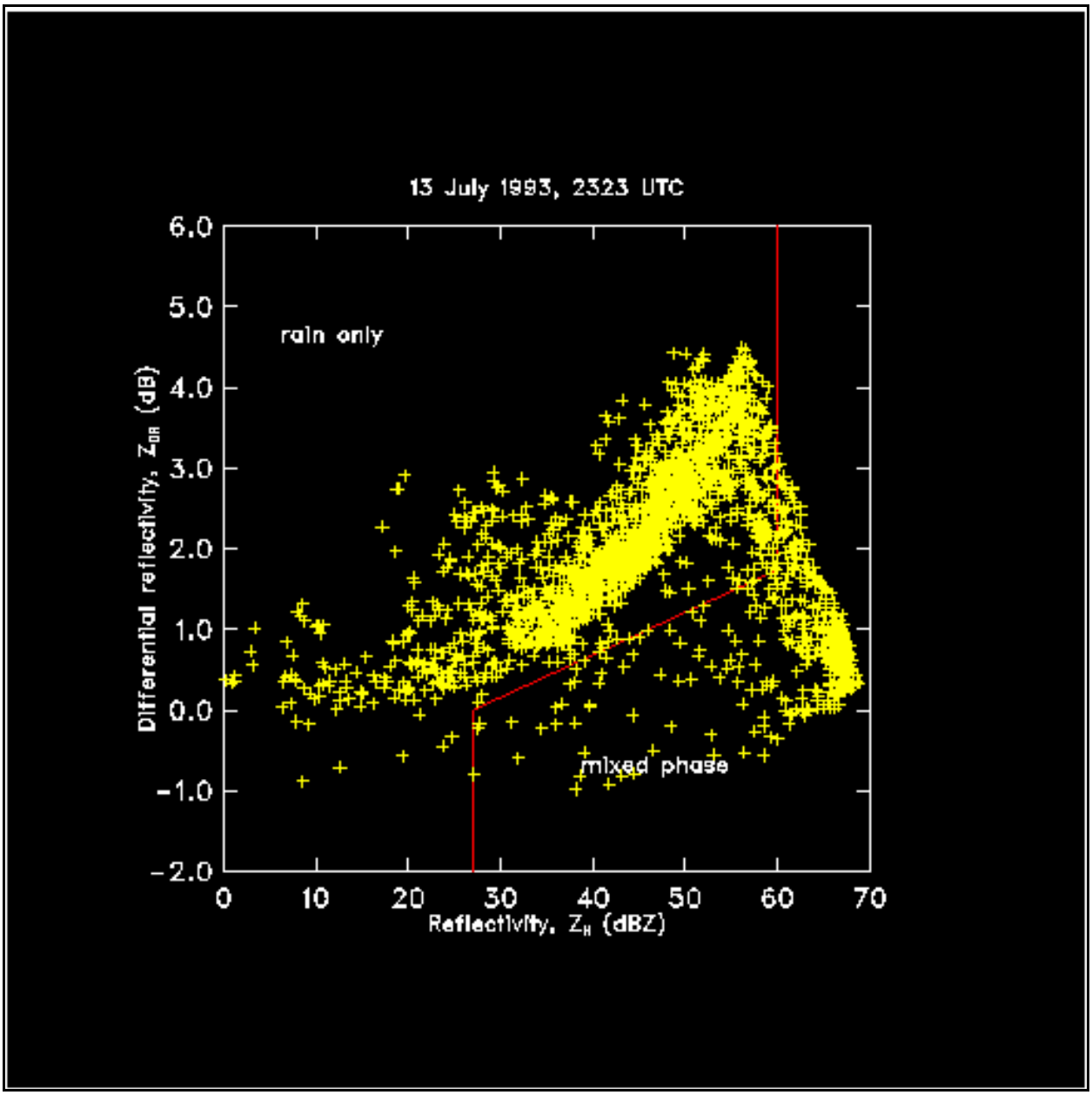

Fig. 2. The distribution of radar reflectivity (Z_h) and differential reflectivity (Z_{DR}) in a hail storm observed in northeastern Colorado.

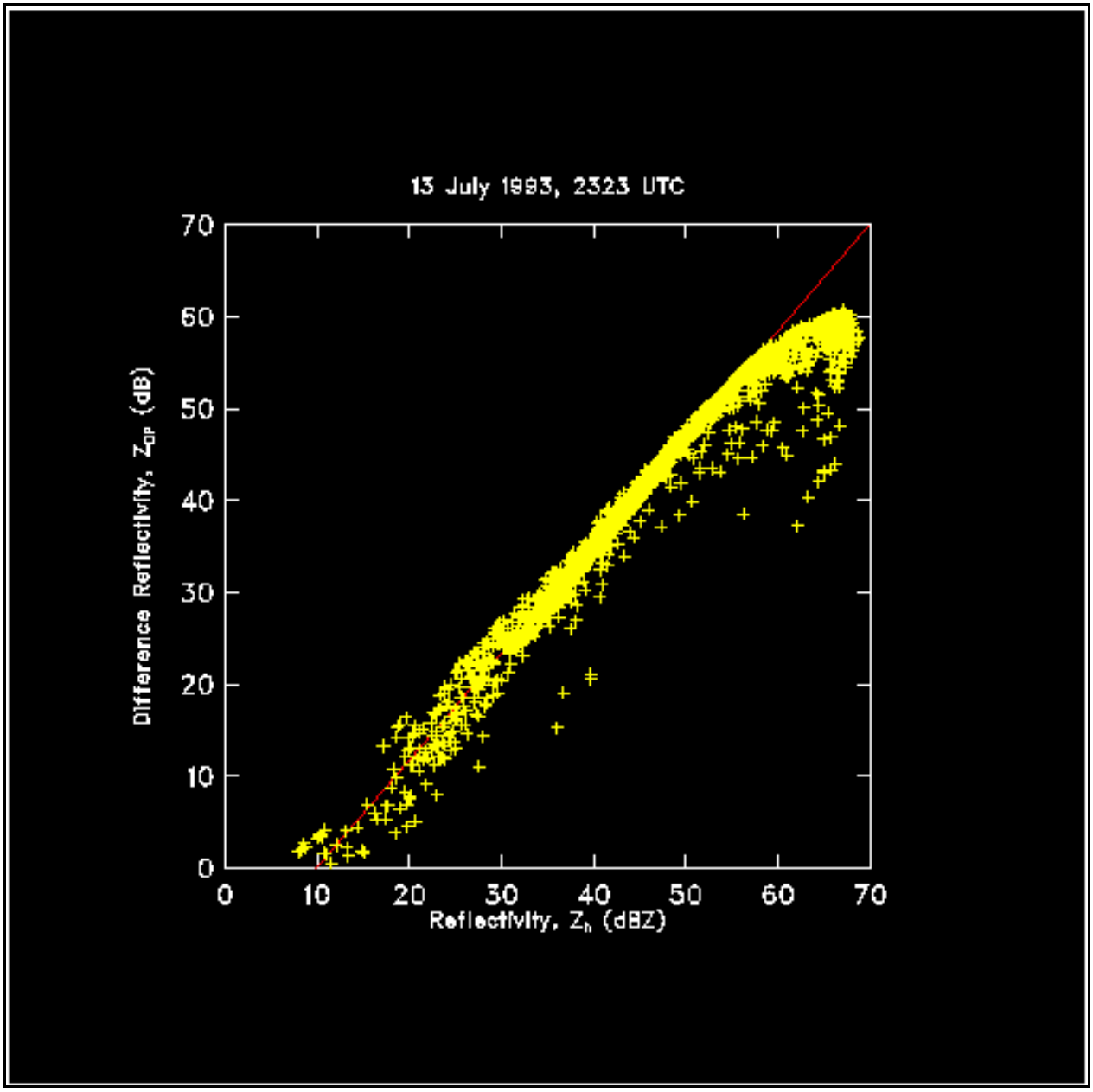

Fig. 3. The distribution of radar reflectivity (Z_h) and difference reflectivity (Z_{DP}) for the storm shown in Fig. 2. The straight line represents a least-squares fit applied to data points with $H_{DR} < -5$ dB.

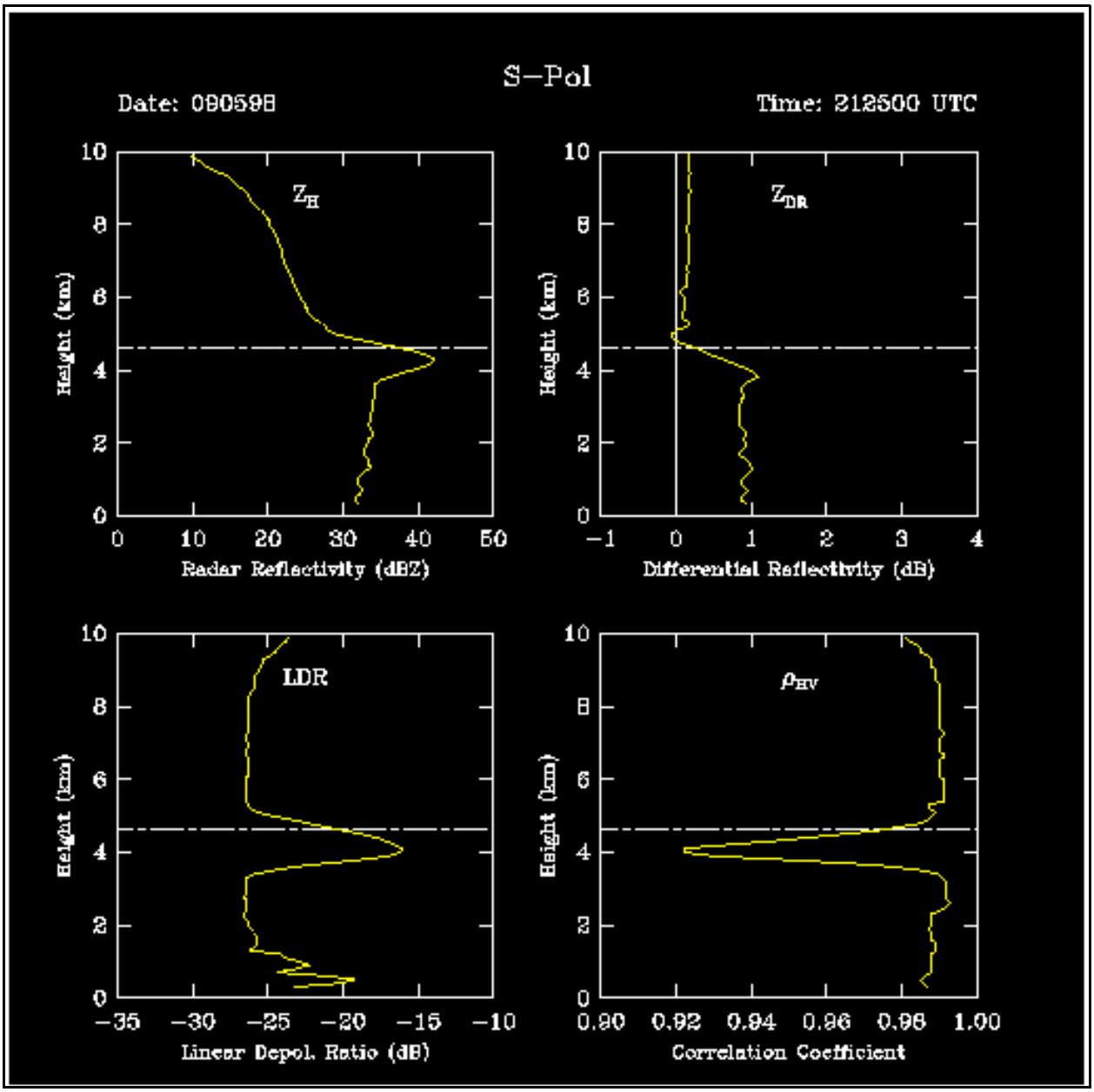

Fig. 4. Profiles of radar reflectivity (Z_H), differential reflectivity (Z_{DR}), linear depolarization ratio (LDR), and correlation coefficient (ρ_{HV}). The freezing level (4.6 km) is shown by a dashed line. The data were collected in east central Florida.

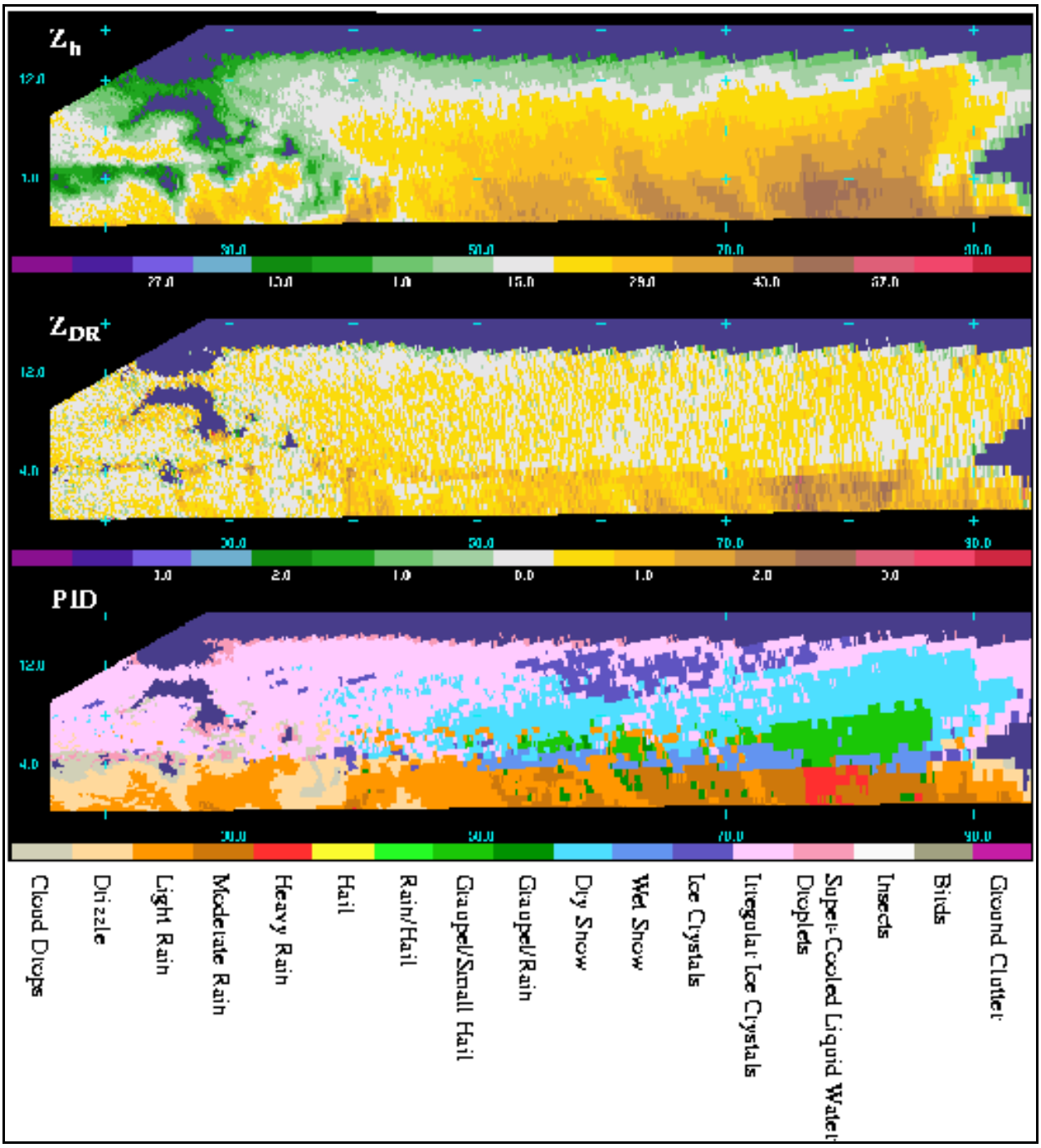

Fig. 5. A vertical cross section through a mature moderate thunderstorm observed in Florida on 19 August 1998. The panels show radar reflectivity (Z_h), differential reflectivity (Z_{DR}), and echo classifications (PID) after Vivekanandan et al. (1999). Distances (tick marks) are in kilometers.